 doi:10.20944/preprints202109.0004.v1

Article

Spirals and Rings in Barred Galaxies by the ROTASE Model

Hongjun Pan

University of North Texas, Denton, Texas 76203, USA; hpan@unt.edu

Abstract: This paper extends the application of the ROTASE model for the formation of spiral arms of disc galaxies, questions and confusions from readers about this model are addressed. The optical trail effect behind the spiral arm rotation is the natural consequence of the model. The morphologies of ring-galaxies are classified into four categories: type I: single ring; type II: 8-shaped double ring; type III: 8-shaped double ring wrapped by a larger outer ring; type IV: single ring without spiral and bar. All four types of ring galaxies can be described by the ROTASE model. The ROTASE model predicts that the false impression of spiral arm rotating ahead of the galactic bar in the galaxy MCG+00-04-051 will change with time, it will look like a normal galaxy with about 30° to 40° bar rotation in the future and the galactic bar ends will look like rotating ahead of the spiral arms with further 10 ° to 15 °bar rotation. The formation of one arm galaxies is due to X-matter at one side of supermassive black hole is much stronger than other side. More evidence is found to support the explanation of the formation and the evolution of the Hoag's object. The possible evolution of spiral pattern of galaxies is illustrated by UGC 6093. The winding of the Milky Way could be tighter in the future based on the ROTASE model.

Keywords: ROTASE model, formation of spiral arms; X-matter; black hole, matter conversion, hydrogen generation, chain-link, single ring; double rings, ring crossing.

1. Introduction

If at the first the idea is not absurd, then there is no hope for it – Albert Einstein. Galaxies are the most dominant celestial massive objects in the universe. It is estimated that the number of galaxies in the universe may be up to 2 trillion [1], and about two thirds of those galaxies are spiral galaxies with very beautiful spiral arms and rings. Spiral galaxies have some common internal structures: a flat differential rotating disc, a stellar bugle, a super massive black hole in the center, spiral arms, a galactic bar or no bar. However, the morphologies of the spiral galaxies vary substantially among them. Hubble was the first to classify the morphologies of the spiral galaxies into different categories called Hubble sequence [2]. Elmegreen & Elmegreen proposed a new classification scheme in which the spiral galaxies can be classified into 12 types according to the number and length of spiral arms [3,4]. It is very important to understand the mechanism of the formation of the spiral galaxies because it is related to the fate of our Milky Way and the universe. Several hypotheses have been proposed in the past. Mcvitte and Payne-Gaoschkin proposed a model based on the Newtonian gravitation laws [5]. The density wave theory (DWT) is the current leading theory in explaining the formation of the spiral pattern proposed by Lin and Shu in 1964 [6,7]. It describes the spiral arm as a quasi-stationary density wave that rotates around the galactic center with a constant pattern speed, but is limited only to the spiral galaxies which have well defined architectural spiral arm patterns such as grand design galaxies, and are only a small portion of all types of galaxies. The DWT cannot explain the formation of spiral galaxies with spurs and branches. The swing amplification model describes the spiral arms as a superposition of many unstable waves, where the spirals generated by the swing amplification are transient and recurrent [8]. Romero-Gomez et. al. proposed a Manifold model in a series of 5 papers to describe the formation of the spiral and ring patterns of galaxies [9-13] In this manifold model, the spirals and rings are developed in the vicinity of Lagragian points near the ends of galactic bars. The stars and interstellar matter circulate along the pipe line guided by the invariant manifolds. Tidal

Preprints (www.preprints.org) | NOT PEER-REVIEWED | Posted: 1 September 2021 doi:10.20944/preprints202109.0004.v1

interactions may cause the formation of spiral structures also as studied by Dobbs et. al. [14]. Dobbs and Baba made detailed reviews about the spiral structure of the galaxies [15]. The author proposed a new model called Rotating Two Arm Sprinkler Emission model in 2019 (for short, ROTASE model) to describe the formation of the spiral galaxies. It was inspired by the morphological similarity between the spiral galaxies and hurricanes and between the spiral galaxies and the rotating two arm sprinkler systems used in watering lawns. A new set of spiral equations was developed and most (if not all) of spiral patterns of galaxies can be simulated. Many special characteristics were also explained by this model. The average pitch angle of the spiral galaxies can be easily calculated after the successful spiral pattern simulation [16-18]. This paper will extend the application of the ROTASE model and address questions and confusions arose since the first publication of this model.

2. Brief description of The ROTASE model and new spiral equations

2.1. Brief description of the ROTASE model

The Rotating Two Arm Sprinkler Emission model can be briefly summarized below and readers may refer the reference paper for the detail description of the model [16-18].

1. A disc galaxy can be treated as an ideal fluid system with flat differential rotation.
2. At the center of the galaxy, the central supermassive black hole (SMBH) converts the gravitational matter to unknow matter with anti-gravitational matter or non-gravitational matter under its extremely unimaginable physical conditions, the property of the unknown matter is unknown, and is named as X-matter for "unknown".
3. The X-matter is emitted by the SMBH in two opposite directions in the disc plane. The X-matter moves in a confined straight route for certain distance, then moves freely which will be dragged by the galactic rotation fluid, the final motion of the X-matter is the combination of the X-matter emission velocity and the galactic fluid rotation velocity.
4. The X-matter will be gradually converted to the hydrogens during its motion, such extra hydrogens increase the local hydrogen density which will promote new star formation and refuel existing local stars, temporally enhances the local luminosity which are the observed spiral arms and the galactic bar.

2.1.2. The new spiral equations

The trajectory of the X-matter can be calculated by the new spiral equations derived from the ROTASE model. The following is the primary master differential equation set:

$$\begin{cases} dx = R_b * \cos(\alpha)\, d\theta = R_b * \frac{y}{\sqrt{x^2+y^2}}\, d\theta \\ dy = R_b * (\rho(\theta) - \sin(\alpha)) d\theta = R_b * \left(\rho(\theta) - \frac{x}{\sqrt{x^2+y^2}}\right) d\theta \end{cases} \quad (1)$$

Where, x and y are the coordinates of spiral arm point in the calculation, precisely speaking, the x and y are the coordinates of X-matter in the calculation. R_b is the half length of the galactic bar, θ is the rotation angle of the galactic bar from the reference axis from which the X-matter is emitted. The parameter ϱ(θ) is defined as the ratio of the X-matter emission velocity V_e (θ) over the flat rotation velocity V_r of the galactic fluid:

$$\rho(\theta) = \frac{V_e(\theta)}{V_r} = f(\theta) \quad (2)$$

The rotation angle θ of the galactic bar can be used as time counting just like the clock in which the rotation angles of the clock hands can be used as time counting, the 90° of the

Preprints (www.preprints.org) | NOT PEER-REVIEWED | Posted: 1 September 2021 doi:10.20944/preprints202109.0004.v1

rotation angle of the minute hand represents 15 minutes of time, i.e., 90° = 15 min. In ROTASE model, the relationship of time t with the rotation angle θ is defined as:

$$t = \frac{R_b}{v_r}\theta \tag{3}$$

The θ in equation (2) represents time. The emission velocity V_e of X-matter can change with time (θ) in any format, so does the ϱ(θ), so the parameter ϱ will be the function of θ with assumption that the flat rotation velocity V_r is constant. The ϱ is a pure number without a physical unit.

The differential equation set (1) can be solved in the polar coordinate system in three different cases:

$$r = \frac{R_b}{1-\rho*\sin(\alpha)} \tag{4}$$

For ϱ > 1:

$$\left(\frac{1}{\rho^2-1}\right)\left\{\sqrt{(\rho^2-1)r^2 + 2rR_b - (R_b)^2} - \left(\frac{R_b}{\sqrt{\rho^2-1}}\right)\ln\left|r\sqrt{\rho^2-1} + \frac{R_b}{\sqrt{\rho^2-1}} + \sqrt{(\rho^2-1)r^2 + 2rR_b - (R_b)^2}\right|\right\} - \left(\frac{R_b}{\rho^2-1}\right)\left(\rho - \frac{1}{\sqrt{\rho^2-1}}\ln\left|\frac{\rho^2 R_b}{\sqrt{\rho^2-1}} + \rho R_b\right|\right) = R_b\theta \tag{5}$$

For ϱ = 1:

$$\frac{\sqrt{2}}{3\sqrt{R_b}}(r + R_b)\sqrt{r - \frac{R_b}{2}} - \frac{2}{3}R_b = R_b\theta \tag{6}$$

For ϱ < 1:

$$\frac{R_b}{(1-\rho^2)^{\frac{3}{2}}}arcsin\left(\frac{(1-\rho^2)r - R_b}{\rho R_b}\right) - \frac{1}{(1-\rho^2)}\sqrt{2rR_b - (R_b)^2 - (1-\rho^2)r^2} - \frac{R_b}{(1-\rho^2)^{\frac{3}{2}}}acrsin(-\rho) + \frac{\rho R_b}{1-\rho^2} = R_b\theta \tag{7}$$

All angles (θ and arcsin) in the equations have the unit of radian not degree. For the equation (4), the maximum value of the sin (α) is 1, therefore, for ϱ < 1, the maximum moving distance of the X-matter from the galactic center is limited, this results in the beautiful spiral-ring pattern with radius of the ring defined by:

$$r(radius\ of\ the\ ring) = \frac{R_b}{1-\rho} \tag{8}$$

For ϱ = 1, the ring size is infinitive, i.e., no ring pattern. For ϱ > 1, the following condition must be followed:

$$\sin(\alpha) < \frac{1}{\rho} \tag{9}$$

The r is unlimited. The differential equation set (1) can be called as the parent spiral equations and the four solutions (4) to (7) can be called as the child spiral equations. The new spiral equations can be named as galactic spiral equations.

The trajectory of the X-matter can be calculated by either the parent differential equation set (1) or the child solution equation set (4) to (7), they both give the same results, the detailed steps for the calculation are described in the references [16 -18], a mini simple computer program can be used to carry such calculations. The calculated x and y have to be rotated backwardly by (-θ) for final spiral plotting with x' and y',

$$\begin{cases} x' = x*\cos(-\theta) + y*\sin(-\theta) \\ y' = -x*sin(-\theta) + y*\cos(-\theta) \end{cases} \tag{10}$$

Preprints (www.preprints.org) | NOT PEER-REVIEWED | Posted: 1 September 2021 doi:10.20944/preprints202109.0004.v1

The critical backward rotation is clearly explained in the reference paper [18]. Euler rotation may be carried out to match the orientation of the galactic disc to the line of the sight. There are many different Euler rotation matrices available, the Euler rotation matrix used here is:

$$R(\varphi\sigma\psi) = \begin{bmatrix} cos\phi\ cos\psi - cos\sigma\ sin\psi\ sin\phi & -sin\psi\ cos\phi - cos\sigma\ sin\phi\ cos\psi & sin\sigma\ sin\phi \\ sin\phi\ cos\psi + cos\sigma\ cos\phi\ sin\psi & -sin\phi\ sin\psi + cos\sigma\ cos\phi\ cos\psi & -sin\sigma\ cos\phi \\ sin\sigma\ sin\psi & sin\sigma\ cos\psi & cos\sigma \end{bmatrix} \quad (11)$$

Questions may arise: why is the proposed X-matter non-gravitational or anti-gravitational? Why is the X-matter emission by the SMBH in the disc plane not vertical or other angles (like the AGN emission)? Well, based on the current physics, the black hole has the super strong gravitational force, any regular gravitational matter inside of the horizon cannot escape from the black hole, therefore, the proposed X-matter must be non-gravitational or anti-gravitational. We know that all galactic bars and spiral arms are in the disc plane of the galaxies, therefore the emission of the X-matter must happen in the disc plane to fit the observations, otherwise, no such ROTASE model can be proposed. We have to make the best conjecture or assumption based on all available observations and data, this is the basic philosophy adopted in all aspects of our society, not like the lottery number picking.

3. The luminosity and the quality of the spiral arms decrease with time or the length of the arms

As the ROTASE model assumed that after the X-matter is emitted from the central SMBH, it moves in a confined route for certain distance, then it moves freely with combined motion of its exited motion and the rotation of the galactic disc fluid, it will be gradually converted to hydrogens during such motion. For simplicity, let us assume that the conversion rate follows the first order, i.e., the rate of X-matter converted to the hydrogens is proportional to the total amount of the remaining X-matter:

$$-\frac{dM}{dt} = KM \quad (12)$$

Where, M is the total remaining X-matter, K is the conversion rate constant. Then,

$$M = M_0 e^{-Kt} \quad (13)$$

M_0 is the initial amount of the X-matter. The total amount of X-matter decreases with time. The hydrogen production rate is proportional to the X-matter conversion rate:

$$\frac{dH}{dt} = kM = kM_0 e^{-Kt} \quad (14)$$

Where H is the amount of hydrogens, k is the hydrogen production rate constant. The hydrogen production rate decreases with time. The extra hydrogen density produced along the motion line by conversion of X-matter gradually decreases, the stars near the motion line receive less and less extra hydrogens, which makes the enhanced luminosity gradually decreasing. The luminosity of the X-matter traveled area will gradually go back to normal after the X-matter passes through due to depletion of the extra hydrogens. The "normal" is the luminosity level before the arrival of the X-matter band, and "gradually going back to normal" will cause the observed optical "trail effect" which is left behind by the X-matter band rotation and can be observed in real galaxies. The first order conversion assumption here is just for illustration purpose, the real case could be more complicate than the first order assumption.

The X-matter moves from inside-out, and hydrogens are created from the X-matter which will refuel the local stars and promote new star-forming during such inside-out

Preprints (www.preprints.org) | NOT PEER-REVIEWED | Posted: 1 September 2021 doi:10.20944/preprints202109.0004.v1

motion. Readers may think that the stars along the spiral arm should present an age gradient from inside-out which timing should match that of the differential velocity between the propagation of the X-matter and the disk rotation velocity. However, this is a misunderstanding. First, this misunderstanding implies that all stars in the galaxies are formed by the hydrogens converted from X-matter. However, in the ROTASE model, the stars in the galaxies already exist before the central SMBH starts to emit the X-matter, and the hydrogens converted from the X-matter only refuel the local stars (which already exist) and make those stars temporarily brighter, the new stars promoted by the extra hydrogens only make small portion of the total stars in the local areas. Second, the hydrogen conversion from X-matter happens across the entire X-matter bands simultaneously, and the star refueling and star-forming promoted by the extra hydrogens happen simultaneously in the entire X-matter band as well. This is why all new stars in the entire spiral arms have similar ages. However, the amount of hydrogens converted from the X-matter decreases along the X-matter band lines (the spiral arm lines), so, the luminosity of the spiral arms sequentially decreases along the spiral arm lines inside-out due to the aging (decreasing the amount) of X-matter. According to the ROTASE model, the X-matter bands (the spiral arms) and the galactic bar rotate together as a "solid" object, but the galactic disc fluid rotates differentially. The newly formed stars are gravitational objects, and do not follow the X-matter band (spiral arm) rotation. They will stay with the galactic disc fluid and rotate with the fluid, will be left behind the rotation of the X-matter bands (the spiral arms), and will start their own evolution sequences. The refueled stars rotate with the galactic fluid, not with the X-matter band. The luminosity of those refueled stars will gradually decrease with gradual depletion of the extra hydrogens refueled, which will cause the observed "trail effect". As the X-matter bands continue rotation, star refueling and new star-forming continue happening in the entire X-matter bands, this completely agrees with the observations that the almost all new star-forming areas are located in the spiral arm regions (except for the nuclear rings close to the galactic center) and new star-forming has a similar (narrow range of) ages in the entire arm areas. This will be further explained in the section 6 with a real galaxy.

Stephen Hawking made a definition about a good theory [19]: *A theory is a good theory if it satisfies two requirements. It must accurately describe a large class of observations on the basis of a model that contains only few arbitrary elements, and it must make definite predictions about the results of future observations*. The conjecture made by ROTASE model will be tested through the rest of the paper with Hawking's criteria.

4. Pitch angle of the spiral galaxies

Pitch angle (PA) is used to measure the tightness of the spiral arms and to characterize the structural morphology of the spiral galaxies. The pitch angle is defined as the angle between the tangent of the spiral arm and the tangent of the circle at the same spiral arm point with its center located at the galactic center. Such tightness is believed to be possibly related to the mass of the SMBH at the center of galaxies; larger pitch angle may reflect smaller mass of SMBH [20-22].

From the above spiral formulas by the ROTASE model, the formula for calculating the pitch angle PA at any point (x', y') of the spiral arm can be derived as following:

$$PA(x',y') = ABS\left\{ arctg\left[\frac{R_b*\rho(\theta)*\cos(-\theta)+\left(1-\frac{R_b}{\sqrt{(x')^2+(y')^2}}\right)*x'}{R_b*\rho(\theta)*\sin(-\theta)-\left(1-\frac{R_b}{\sqrt{(x')^2+(y')^2}}\right)*y'}\right] - arctg\left[-\frac{x'}{y'}\right]\right\} \quad (15)$$

The first *arctg* of the formula (15) is the tangent angle of spiral arm at location (x', y'), the second *arctg* of the formula (15) is the tangent angle of the circle at the same location (x', y') with center at the galactic center. The PA(x', y') is the absolute (ABS) value of the

Preprints (www.preprints.org) | NOT PEER-REVIEWED | Posted: 1 September 2021 doi:10.20944/preprints202109.0004.v1

difference of the two tangent angles, sometimes, a sign of positive or negative pitch angle is used to reflect the chirality; if the value is greater than 90°, then the pitch angle will be the result of subtracting the value from 180°. When the spiral pattern of the galaxy can be satisfactorily fit by the ROTASE model, the pitch angle will be easily calculated with equation (15). The author also proposed a new averaging method in a previous paper [18] to more fairly average the pitch angles from all different parts of the entire galaxy, this new average method is called Spiral Arm Length Weighted Average pitch angle, for short, SALWA pitch angle PA(w). The "w" means "weighted", the PA(w) is defined as:

$$PA(w) = \frac{1}{L}\sum PA_i * (dL)_i \tag{16}$$

Where, the PA_i is the pitch angle of i^{th} data point, $(dL)_i$ is the spiral arm length at the i^{th} data point, L is the total length of the spiral arm:

$$L = \sum (dL)_i \tag{17}$$

The proposed SALWA pitch angle (16) is based on the fact that a different pitch angle data point PA_i in the calculation represents a different length of the spiral arm section. This is true for all other commonly used spiral formulas (Archimedean, logarithmic, and Ringermacher-Mead spirals); therefore, the weighting on the length of the spiral arm section will more fairly reflect the contribution of different parts of the spiral arm for the entire galaxy. The calculation of the pitch angle based on the ROTASE model cannot quantify the error because it is based on the spiral line fitting, not based on the statistical analysis.

5. Theoretical spiral patterns calculated by the new spiral equations

Figure 1 lists 10 different spiral patterns calculated by the spiral equations above with different parameter ϱ, those spiral patterns are very common in the observed galaxies.

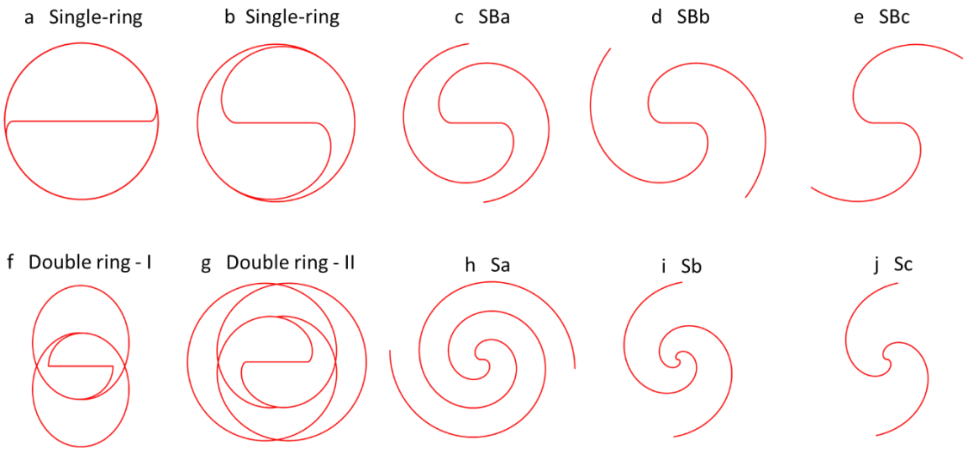

Figure 1. common galactic spiral patterns produced by the ROTASE model. First row a: ϱ=0.1, single spiral ring, b: ϱ = 0.5, single spiral ring; c: ϱ = 0.7, SBa; d: ϱ = 1.4, SBb,; e: ϱ = 2.5, SBc. Second row f: ϱ = 0.6*exp(-0.0001*(θ-360)²), double ring; g: ϱ = 0.6*exp(-0.00001*(θ-450)²), double ring; h: ϱ = 6, Sa; i: ϱ = 6 + 0.05*θ, Sb; j: ϱ = 6+0.08*θ, Sc.

Figure 1a is the single spiral ring pattern with constant ϱ = 0.1. This is a very tight ring with little spiral structure. Figure 1b is the single spiral-ring pattern with ϱ = 0.5. It has a good portion of spiral structure, and one can see that the spiral portion will increase with the parameter ϱ. Figure 1c is a spiral pattern with constant ϱ = 0.7. Such a pattern is classified as SBa pattern according to Hubble sequence. It is a barred spiral with tight

Preprints (www.preprints.org) | NOT PEER-REVIEWED | Posted: 1 September 2021 doi:10.20944/preprints202109.0004.v1

winding; however, with this ϱ value, it should be a spiral ring pattern if the spiral arm extends longer, so it is a truncated spiral ring pattern. Figure 1d is the SBb pattern in Hubble sequence with ϱ = 1.4. It is a barred spiral with loose winding. Figure 1e is the SBc pattern in Hubble sequence with ϱ = 2.5. It is a barred spiral with more open winding. One can see that the spiral winding will be looser and more open with increase of ϱ. Figure 1f is a double ring pattern in which the ϱ changes with time following the Gaussian equation with maximum value of ϱ happened at 360° galactic bar rotation time ago from now. This means that peak emission of the X-matter by the central SMBH happened 360° galactic bar rotation time ago. This type of double ring spiral pattern shows an 8-shaped double ring structure. Figure 1g is the double ring spiral pattern in which the ϱ changes with time following the Gaussian equation with maximum value of ϱ happened at 450° galactic bar rotation time ago from now. This type of double ring shows an 8-shaped inner structure wrapped with larger outer rings, and the spiral windings are much more complicated. The double ring patterns are very interesting and will be addressed later in more detail. Figure 1h is the Sa pattern in Hubble sequence with ϱ = 6. It is a tight winding and unbarred spiral. Figure 1i is the Sb pattern in Hubble sequence with ϱ changing linearly with time. It is a loosely winding and unbarred spiral. Figure 1j is Sc pattern in Hubble sequence with ϱ changing with time more aggressively. The unbarred spiral galaxies may still have bars, but the length of the bars is small compared to the size of the galactic discs and cannot be recognized easily due to bright central bugle and the nuclear ring with very active new stars forming.

6. Galaxy J101652.52-004630.0 with constant X-matter emission

The spiral galaxy J101652.52-004630.0 is a well-defined grand-design spiral galaxy with two short and very clean spiral arms shown by the original image in Figure 2 left without spurs, branches and random noisy spots to spoil the image of the galaxy. The two spiral arms have perfect central symmetry, and it will be a good example to be studied by the ROTASE model. To the author's limited knowledge, this galaxy is relatively new to us, and has not been studied previously by other people. The spiral pattern of this galaxy was nicely simulated in a previous paper by the ROTASE model shown in Figure 2 right with solid red (north arm), orange (bar) and yellow (south arm) lines with a constant parameter ϱ = 2.5 and 95° of total bar rotation angle. It is a very loose open spiral galaxy and should be a SBc type galaxy in Hubble sequence. This image is almost a face-on image according to the Euler angles. This galaxy will be revisited in this paper with exploration of more details by the ROTASE model.

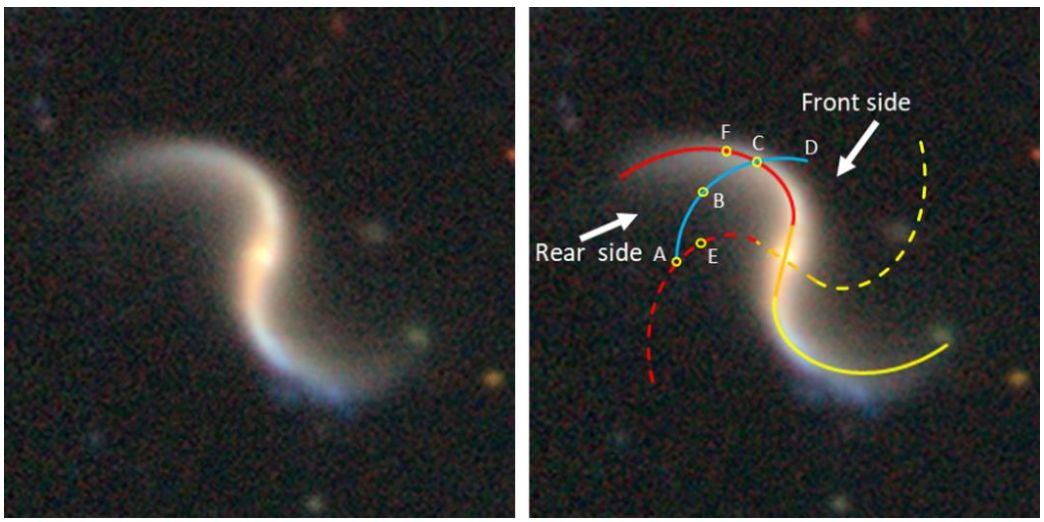

Figure 2, the galaxy J101652.52-004630.0, left: the original image, right: simulation (red and yellow) of by ROTASE model, ϱ = 2.5, Euler (14,5, 0)

Preprints (www.preprints.org) | NOT PEER-REVIEWED | Posted: 1 September 2021 doi:10.20944/preprints202109.0004.v1

If we inspect the original image carefully, we can find: 1. The luminosity sequentially decreases along the spiral arm lines from the end of the galactic bar to the end of the visible arms. 2. It rotates clockwise, the front rotation side of the spiral arms has a very clean and sharp edge where the luminosity (surface brightness) decreases sharply; by contrast, the rear side is very blurry/dispersed, and the luminosity decreases slowly. The surface luminosity along the north spiral arm line (red) can be extracted as shown in Figure 3.

Figure 3, the surface luminosity changes along the spiral arm line in galaxy J101652.52-004630.0

One can see that the surface luminosity steadily decreases along the spiral arm line from the end of the bar to the end of the visible arm line. The decrease of the luminosity along the spiral arm line can be well fitted by an exponential decay function:

$$y = 109.16 * \exp(-0.0009 * x) \quad (18)$$

This matches equations (13) and (14) well.

Preprints (www.preprints.org) | NOT PEER-REVIEWED | Posted: 1 September 2021 doi:10.20944/preprints202109.0004.v1

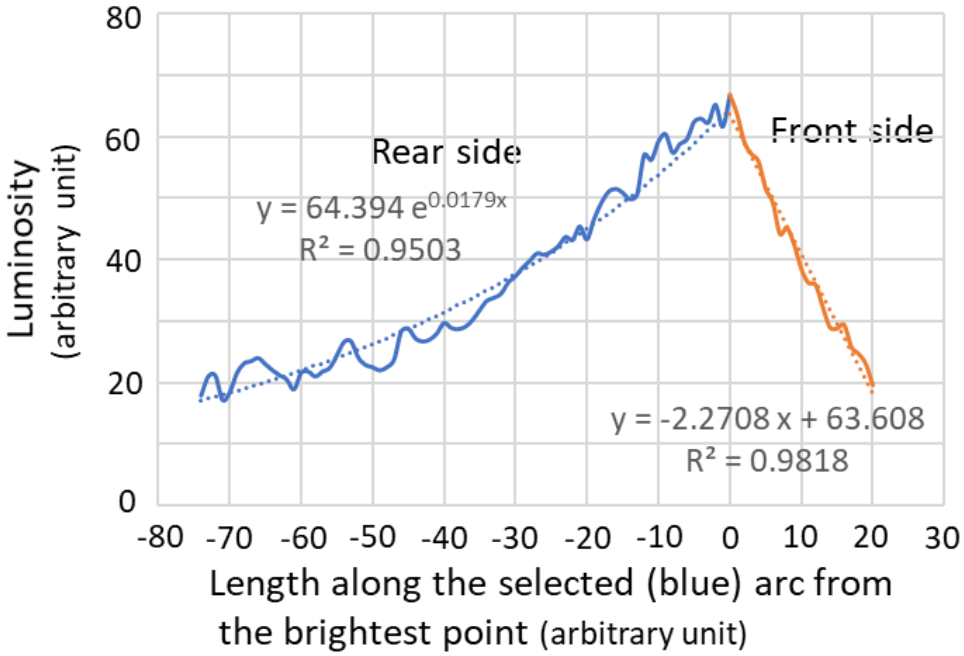

Figure 4, the surface luminosity changes along the selected blue arc in the Figure 7.

Figure 4 shows the changes of the surface luminosity along the selected blue arc (a section of a circle) from points A to D in Figure 2 right. The cross point labeled with letter C by the red spiral arm and the blue arc has the highest luminosity, which is defined as reference point 0 in the horizontal axis in Figure 4. For simplicity, assume that the galactic disc has a perfect differential flat rotation, and all stars and galactic matter rotate along the perfect circular lines with their radii. Based on the ROTASE model, the spiral arms and the galactic bar rotate together as a "rigid" solid structure, but the stars and other galactic matter rotate along the circular lines with their own differential rotation patterns. The spiral arm lines along the red and the yellow lines have the highest luminosity, which means that the density of X-matter is highest with the highest density of hydrogens converted. The stars in these line areas will be refueled with more hydrogens than any other areas and new star-forming will be more active than any other areas. This happens across the entirety of the X-matter band lines simultaneously. Therefore, all new stars formed in the arm lines have similar (narrow range of) ages. Due to the fact that the stars and new-born stars are gravitational, they will follow the disc fluid to rotate along the circular lines. The solid red and yellow spiral lines in Figure 2 right show the current location of spiral arms; the galaxy rotates clockwise. Therefore, at some time ago (possibly millions of years ago), spiral arms were shown in dashed red and yellow lines in Figure 2 right. The local stars in location A at that time received extra hydrogens and new stars were forming at the location A; the luminosity at location A was the highest at that time. However, as the X-matter band keeps spirally moving forward, the stars and the new-born stars at the location A also rotated along the circular (blue) line, but is behind the rotation of the X-matter band. When the X-matter band moves to its current location, the stars and new-born stars originally at the location A may have arrived at the location B with less luminosity due to gradual depletion of the extra hydrogens. Therefore, there is a luminosity gradient from the current location C to the location A along the circular blue line. Beyond the location A, the luminosity is back to normal level as all extra hydrogens are depleted. This is the "trail effect" as mentioned above. The trail effect is a natural consequence of the ROTASE model. The blue line (rear side) in Figure 4 is the luminosity extracted along the blue circular arc of the Figure 2 right from the cross-point C to A. The luminosity change along this arc can be fitted by an exponential decay function:

Preprints (www.preprints.org) | NOT PEER-REVIEWED | Posted: 1 September 2021 doi:10.20944/preprints202109.0004.v1

$$y = 64.5 * \exp(-0.018 * x) \quad (19)$$

Such exponential decay dependence suggests that the depletion of the extra hydrogens may follow the first order consumption rate overall.

One has to keep in mind that as the X-matter band moves spirally outward, the X-matter originally located at location A at millions of years ago has arrived at location F now, not at C. The amount of X-matter gradually decreases along a moving line from A to F. So at F, less hydrogens will be converted, and the local stars at F will receive less extra hydrogens and there will be less new stars formation. The luminosity will also be weaker. The X-matter at the location C is not the same X-matter at location A, it is from "younger" X-matter at the location E which was closer to the galactic center in the past. The X-matter at F and C produce hydrogens at the same time and promote new star-forming at the same time. This explains why the newly formed stars in the entire spiral arm have similar (narrow range of) ages and should clarify the misunderstanding.

The orange line in Figure 4 is the luminosity of the front side of the red spiral arm line in Figure 2 right along the blue circular arc C to D. The luminosity linearly decreases sharply compared to the rear side. Such sharp decrease reflects that the sharp front edge of the spiral arm is the sharp edge of the X-matter band with no trail effect as expected by the ROTASE model.

7. Galaxy M51 with two different X-matter emissions

The Galaxy M51 is a famous whirlpool galaxy with a grand design structure shown in Figure 5, each arm has two very distinguishable spiral structures simulated in a previous paper by the yellow lines and the red lines, respectively. Overall, the two arms have almost perfect central symmetry except for the area indicated by the white arrow in which it is not fitted well. It is a good example for illustration of X-matter emission behavior change by the central SMBH and the central symmetry of the galaxy being damaged by unsymmetrical strong gravitational interaction, so it will be revisited here.

Based on the proposed ROTASE model, the formation of the two distinguishable sections of each spiral arm is due to the central SMBH in M51 emitting the X-matter with two very different emission behaviors as shown in Figure 5. From the galactic bar rotation angle time 485° to 610° in the past from now, it emitted the X-matter to produce the yellow line spiral arm sections with parameter ϱ following the equation:

$$\rho = 0.00088 * (\theta - 535)^2 + 11.704 \quad (20)$$

However, from the galactic bar rotation angle time 485° in the past to now, the central SMBH has been emitting the X-matter to produce the red line spiral arm section with parameter ϱ flowing the equation:

$$\rho = 1.1 * (1 + 0.024 * \theta) \quad (21)$$

The equations (20) and (21) indicate that the X-matter emission velocity in the past gradually decreased, then, at rotation angle 535° time from current, the X-matter emission increased for short period of time (about 50° rotation time), then, it has been steadily decreasing up to today [16]. We will see more cases with the sudden change of the X-matter emission behaviors by central SMBHs in later sections.

Preprints (www.preprints.org) | NOT PEER-REVIEWED | Posted: 1 September 2021 doi:10.20944/preprints202109.0004.v1

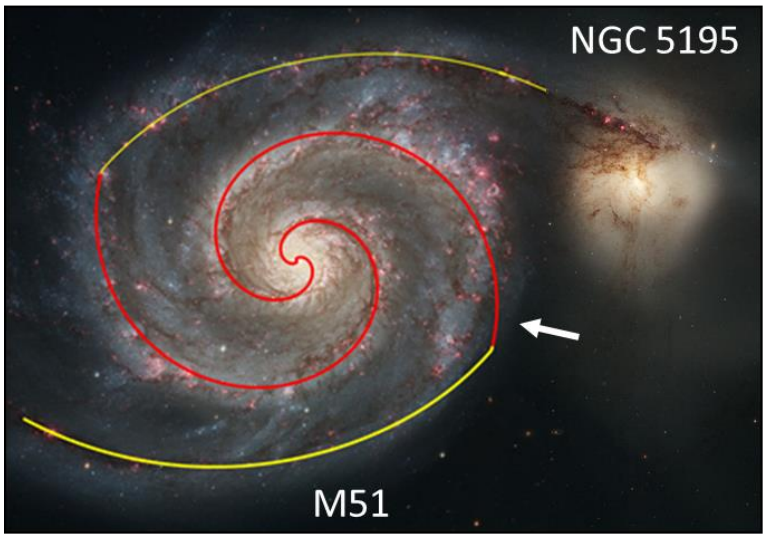

Figure 5, Galaxy M51 and spiral pattern simulation by ROTASE model, Euler(13,0,0)

M51 has a companion galaxy NGC 5195 shown in the upper right. In the tidal interaction model, the spiral arms are the result of tidally induced kinematic density 'waves' or density patterns, which wind up slowly over time [14]. However, this tidal induced mechanism for the formation of spiral arms with perfect central symmetry is realistically implausible, because the intensity of such tidal interaction by the gravitational force between the two cosmic scaled large objects is extremely (central) unsymmetrical. The top yellow arm of M51 is extended to its companion galaxy NGC 5195 by the strong gravitational force; the morphology of the lower arm section pointed by the white arrow is changed by the NGC 5195 with the strong gravitational force; and the other side of spiral arm is not affected due to its distance from NGC 5195. The two galaxies are constantly moving, and the distance between the two galaxies are constantly changing. Realistically, it is hard to believe that such unsymmetrical interaction can produce the spiral arms with perfect central symmetry in the M51 galaxy. It is more reasonable to believe that the spiral structure of the M51 was formed with perfect central symmetry long before the two galaxies approached each other, so the unsymmetrical tidal interaction between the two galaxies damages the central symmetry.

8. Galaxy MCG+00-04-051 with broken spiral arm connection from galactic bar ends

In general, the spiral arms are normally bound with the ends of galactic bars. From the M51 above we already see that the X-matter emission by the central SMBH may change in any format and at any time. This model predicts that when the X-matter emission stops, the arms will disconnect from the ends of the galactic bar, the bar still rotates and the arms still swirl outwardly, rotation gaps between the arms and the ends of the bar occur, such gaps increase with bar rotation with a pattern in which the spiral arm rotates behind of the galactic bar as shown in Figure 6 left. However, in a previous study by Seigar and James [23], such gaps were believed due to the arms moving (rotating) ahead of the bar as illustrated in Figure 6 right. It is found that the very unusual pattern of the galaxy MCG+00-04-051 perfectly matches the predict by the ROTASE model shown in Figure 7a. Such perfect matching is the critical evidence as a solid support for this model.

Preprints (www.preprints.org) | NOT PEER-REVIEWED | Posted: 1 September 2021 doi:10.20944/preprints202109.0004.v1

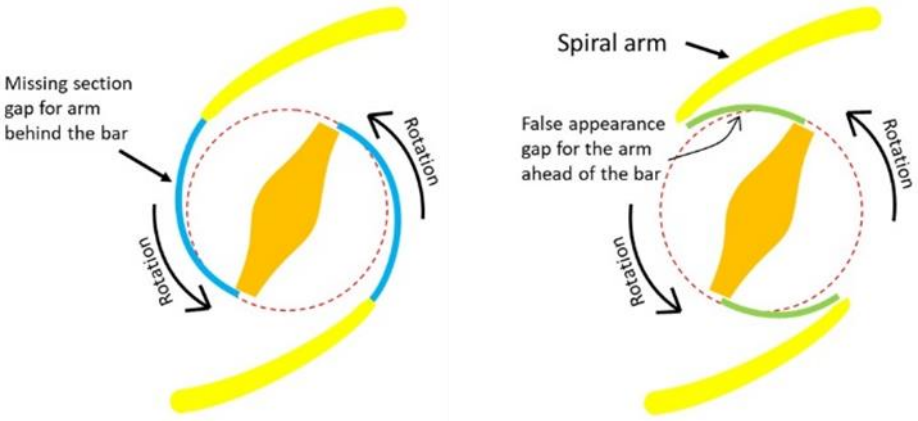

Figure 6. Left: arms rotating behind the bar; right: false appearance of arms rotating ahead of the bar.

Figure 7a is the original image of the galaxy MCG+00-04-051, it is also called SDSS J011430.80+001928.3. The unusual pattern was studied by the ROTASE model in detail in reference [17]. It will be re-visited here with brief description of the spiral pattern by the ROTASE model, and possible patterns in the near future will be predicted by the ROTASE model. This image is a face-on image with spiral arms having perfect central symmetry, the two spiral arms are apparently not connected to the ends of the galactic bar with a strong visual instinctive impression that the spiral arms rotated ahead of the galactic bar. The spiral pattern can be nicely simulated by the ROTASE model shown in Figure 7b with the following parameter ϱ equation:

$$\rho = 0.08*(1+0.015*\theta) \quad (22)$$

However, if we inspect the image carefully, we can find that one arm is still connected to the end of galactic bar with the weak but still clearly visible spiral section indicated by the red dash line in Figure 7b. The inner arm end A was generated at the bar end C, at the time when the A was formed at bar end C, the emission of the X-matter was significantly reduced but was not completely terminated, there was still small amount of X-matter exited from the bar end C, so the arm continued to be formed, which are evidenced with dramatically reduced but still visible spiral arm from A to C in the original image and as simulated by the thin red dash line. However, for the yellow line spiral arm, the arm was formed from E to D in time sequence, and it was terminated at the D without continuing to the end B of the galactic bar. This indicates that the X-matter emission at D was completely stopped or at least the arm in this DB section is so weak and not visible in this image. So, the weak spiral arm section AC is the clear key support for the ROTASE model and proves that the arm end D is behind the bar end B, not ahead of the bar end C. Although, the distance from D to C is much smaller than the distance from D to B, and gives a false impression that D is ahead of C, such false impression will be certainly accepted without question if the weak AC spiral section does not exist. The total rotation angle (equivalent to the evolution time) of the bar for the formation of the arm section AC and the missing arm section DB is 235 degrees. In reality, all other models cannot explain the morphology of this galaxy. Based on the manifold model, the spiral arms started at the L1 and L2 Lagrangian points which are located at the straight line of galactic bar and close to the ends of the galactic bar [10], however, in this galaxy, the "starting" points A and D of the arms are not at the L1 and L2 points, and do not match this model; how does this manifold model explain the weak but still visible arm section AC? Density Wave Theory cannot explain this phenomenon either.

Preprints (www.preprints.org) | NOT PEER-REVIEWED | Posted: 1 September 2021 doi:10.20944/preprints202109.0004.v1

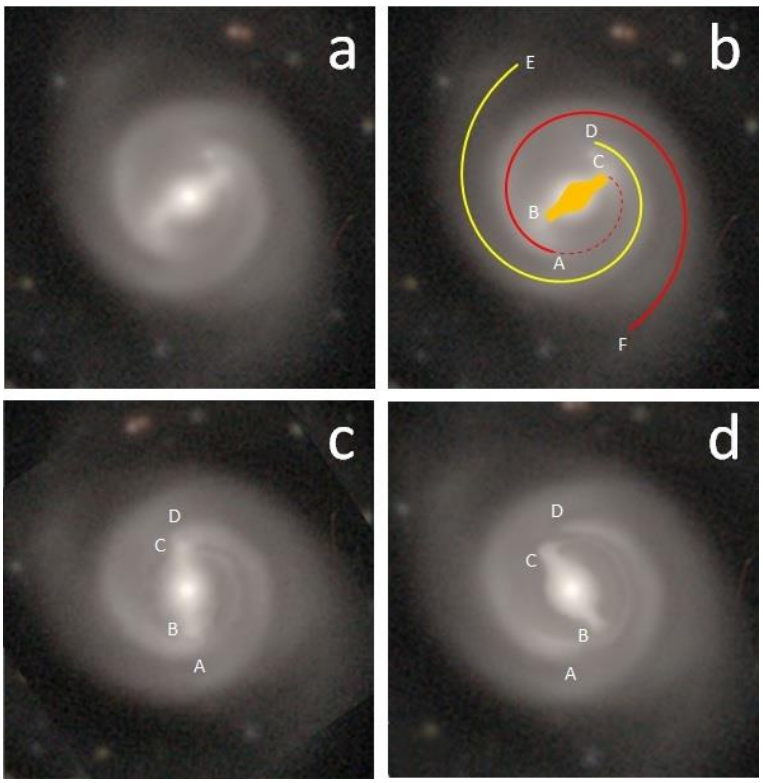

Figure 7. Left: the original image of galaxy MCG+00-04-051; middle: Simulation by the ROTASE model, Euler (-57, 0, 0), right: possible pattern in near future.

The ROTASE model predicts that if the current trend continues, the gap between A and B as well as the gap between C and D will gradually decrease with time. In about 30° to 40° of galactic bar rotation, the bar end C will catch up the end D of spiral arm and the bar end B will catch up the end A of spiral arm. The ends of the bar and the ends of spiral arm will line up in a straight line A-B-C-D, the spiral arm end A will look like it could be connected to the bar end B, the spiral arm end D will look like it could be connected to the bar end C if the gap between A and B as well as the gap between C and D are close enough. The image of the galaxy will look like a "regular" spiral galaxy as shown in Figure 7c, which will give a false impression. In this scenario, without referring to the ROTASE model, it would be laughed at if someone says that the spiral arm AF is originated from bar end C and the spiral arm DE is originated from bar end B. When the bar continues to rotate, the galactic bar will overpass the A and D, for another 10 to 15 degrees rotation, the galactic bar will be ahead of the ends of spiral arms as illustrated in Figure 7d. However, if one believes that the spiral arms rotate ahead of the galactic bar in the original image Figure 7a, then, it will predict that the gap between A and B and the gap between C and D will increase with time for the near future. Readers may make their own judgements for which prediction is reasonable. The author feels confident that patterns shown in Figure 7c and Figure 7d will certainly occur in the future if no dramatically exceptional event happens. If we use the galactic bar rotation velocity of Milky Way as a reference, 30° to 40° rotation takes about 10 to 13 million years. 10 to 13 million years is a fleeting moment in the evolution time scale of the universe, but is too long compared to our human history. Such predictions are realistically not observable in the foreseeable future. The galaxies with patterns similar to Figure 7c and Figure 7d should exist in the universe, which may be already in the database or to be detected in the future.

The galaxy NGC 4548 has the same morphology as the MCG+00-04-051. It has an apparent broken connection of the spiral arms from the bar ends in an image with low quality shown in Figure 8 left, but the image with high quality clearly shows that the arm A is connected to the bar end with a weak and still visible spiral arm. The arm B is not

Preprints (www.preprints.org) | NOT PEER-REVIEWED | Posted: 1 September 2021 doi:10.20944/preprints202109.0004.v1

connected to the other bar end as shown in Figure 8 right, and it was studied in detail in the reference [17].

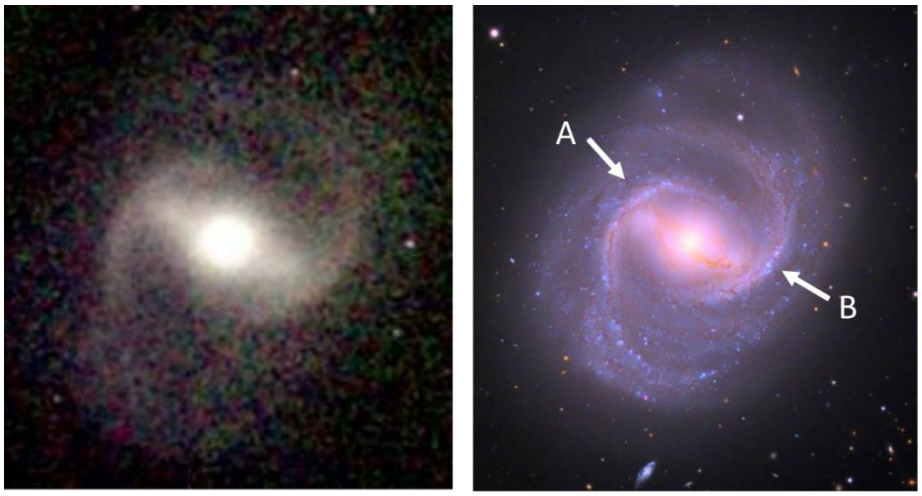

Figure 8, Left: the image of NGC 4548 with low quality; right: image of NGC 4548 with high quality.

9. Galaxies with rings

Galaxies with spiral rings are very popular and can be classified into four major types based on the significant difference of the morphologies. Type I: single ring; type II: 8-shaped double ring; type III: 8-shaped double ring wrapped by a larger outer ring; type IV: single ring without spiral and bar. All four types of ring galaxies can be described by the ROTASE model.

9.1. *Type I: Galaxies with a single spiral ring pattern*

The image of the galaxy CGCG 119-82 on the left of Figure 9 shows almost a perfect round ring with strong bar without the visible spiral structure. It may be classified as a barred lenticular galaxy which contains a large disc without spiral arms. It is a face-on image, and can be simulated nicely by the ROTASE model with $\varrho = 0.1$ as shown in Figure 9 right. Furthermore, the simulation with other small ϱ values (< 0.15) will also show the same result because the ring and the bar ends are close enough and merged together by the blurry optical effect. Based on the ROTASE model, such a pattern is the result of weak X-matter emission (low ϱ value means low X-matter emission velocity). It still has the spiral structure which is hidden under the what looks like a combined ring and bar ends. Because the space between the ring and bar ends is too short to be seen, the direction of the galactic rotation is unknown from the image.

Figure 9, Left: the original image of CGCG 119-82; right: the simulation by ROTASE model, $\rho = 0.1$, Euler (60,0,0)

Preprints (www.preprints.org) | NOT PEER-REVIEWED | Posted: 1 September 2021 doi:10.20944/preprints202109.0004.v1

The spiral structure of the spiral ring galaxies will increase with the value of ϱ and will be more visible as shown in Figure 10.

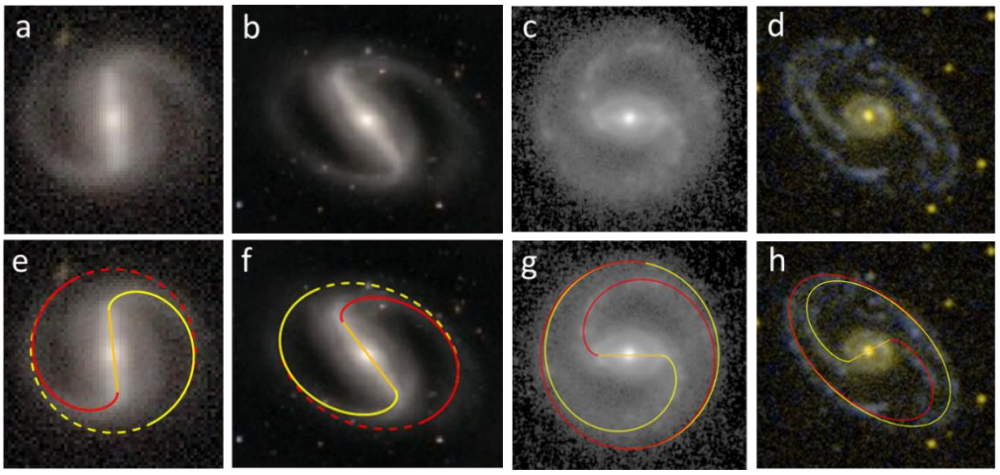

Figure 10, First row are the 4 original images of galaxies with single spiral-ring patterns: a: unknown-name ring 1 from reference [24], b: unknown-name ring 2 from reference[24], c: ESO 325-28; d: NGC 2273

Second row are the images with simulations by the ROTASE model for each related original galaxies in the first row, e: ϱ = 0.5, Euler(6,0,0); f: ϱ = 0.5, Euler(-25,40, 55); g: ESO 325-28, ϱ = 0.65; h: NGC 2273, ϱ = 0.6, Euler (-43, 57, 80).

The images of unknown-name ring 1 and ring 2 galaxies in Figure 10a and 10b are duplicated from reference [24]. The original images show tightly wound open (not closed) spiral patterns which may be classified as SBa type galaxies. However, in Figure 10a and 10b, when the visible spiral arms are simulated by the solid red and yellow lines with constant parameter ϱ =0.5, this results in a single spiral-ring pattern if the visible arms are extend longer shown by the dashed red and yellow lines. Therefore, the two galaxies are concluded to have a truncated single spiral-ring pattern due to the decay of the luminosity along the arm line from the end of galactic bars. The density and the age of the stars along the circle of spiral arm do not cause such decay in luminosity, because the density and age of the stars in the circle are more or less the same. The density wave theory explains the ring formation as resonance of a density wave in this radius, but such resonance cannot explain the gradual decrease of the luminosity along the arm lines. The ROTASE model seems to have a more reasonable explanation that the gradual decrease of the luminosity along the arm lines is only caused by the gradual decrease of hydrogen conversion by the X-matter along the circle of spiral arm lines or "aging" of the arms. The ESO 325-28 galaxy shows a nice face-on single spiral-ring pattern and the NGC 2273 shows a nice single spiral-ring pattern with a large inclination angle. Both the ESO 325-28 and NGC 2273 show a significant spiral structure.

The radius of the rings will follow equation (8) and will increase non-linearly with the ϱ values. Figure 11 shows the single spiral-ring patterns with four different ϱ values; when ϱ =1, the radius is infinite, i.e., no ring. However, in reality, galaxies with only less than 2 windings of spiral arms are observed. Most galaxies have half to one loop winding as marked by "X" in Figure 11 for ring pattern with ϱ = 0.8. The spiral arms beyond "X" are not visible due to the fade away with the decrease of the hydrogen conversion from the X-matter (the amount of X-Matter decreases). These galaxies will have truncated spiral-ring patterns, and will be classified as SBa or SBb patterns in Hubble sequence. In the classical theory of the stellar dynamics of spiral galaxies, the radius of the spiral arms (the size of the galaxies) may be limited by ¼ Lindblad resonance [25]. Beyond ¼ Lindblad

Preprints (www.preprints.org) | NOT PEER-REVIEWED | Posted: 1 September 2021 doi:10.20944/preprints202109.0004.v1

resonance, the disc is not stable, and the spiral arms will not be stable also. However, such a limitation cannot explain the gradual decay of luminosity along the circular line of the spiral arms of the spiral ring galaxies like Figure 10a and 10b.

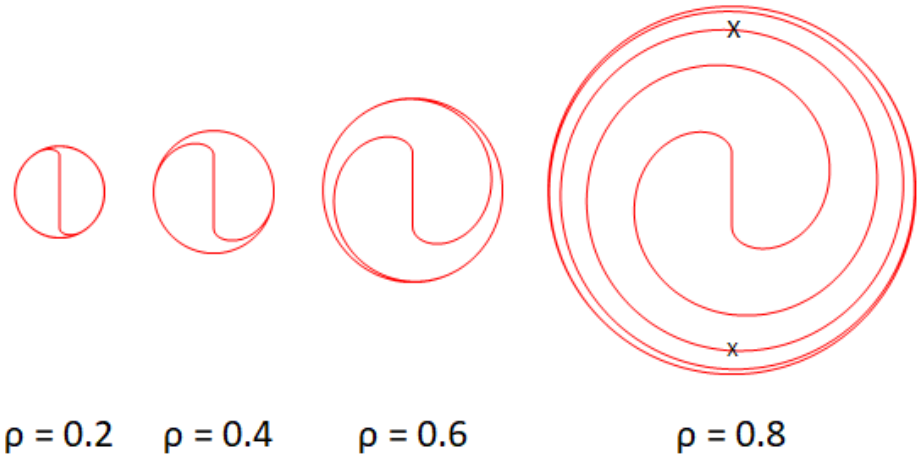

Figure 11, the ring size of the galaxies changes with the parameter ρ.

9.2. *Type II: Galaxies with 8-shaped double spiral ring patterns*

Figure 12 shows 4 galaxies with 8-shaped double ring patterns, NGC 7098, UGC12646, J1015701 and NGC 2665. The upper row are the original images and the lower row are the simulations by the ROTASE model corresponding to their original images above. The parameter ϱ of this type double ring patterns follows the general Gaussian equation:

$$\rho = \rho_0 * \exp\left(-k * \left(\theta - \theta_p\right)^2\right) \quad (23)$$

The ϱ_0 is the maximum value of ϱ; k is a constant controlling the width of the Gaussian profile; θ_P is the angle (time) in the past from now, and at θ_P the X-matter has the peak emission.

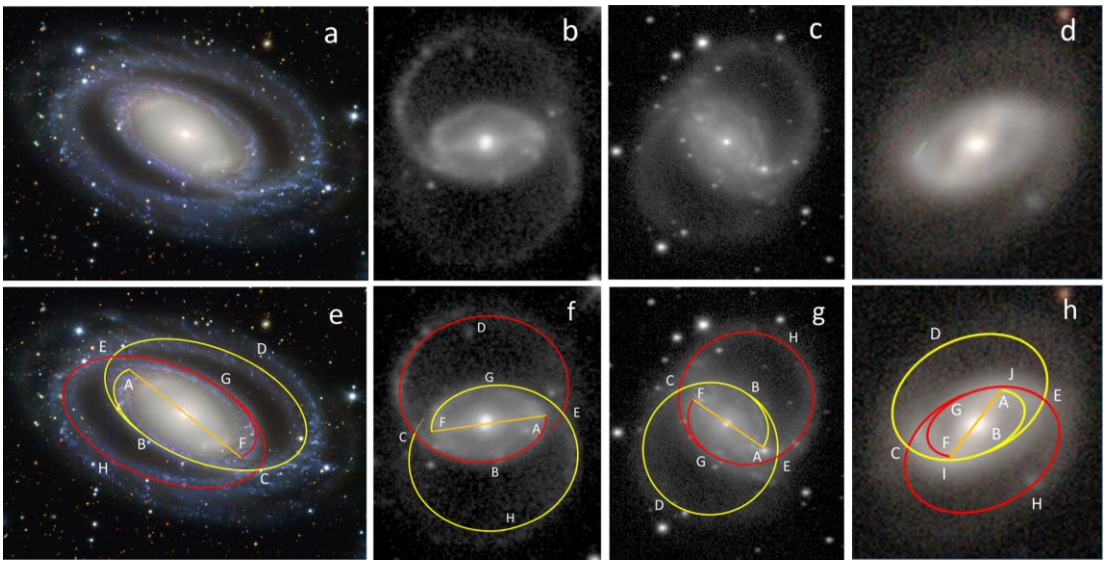

Figure 12, four galaxies with 8-shaped double ring pattern;
Top row is the original images, a: NGC 7098, b: UGC12646, c: NGC 2665, d: SDSS J015701.50-001644.4. Lower row is the simulations for each original image above. e: NGC 7098, Euler(25,65,25); f: UGC12646, Euler(8,59,0); g: NGC2665, Euler (35,35,0); h: SDSS J015701.50-001644.4, Euler(-22,-55,45).

Preprints (www.preprints.org) | NOT PEER-REVIEWED | Posted: 1 September 2021 doi:10.20944/preprints202109.0004.v1

Figure 12a is the original image of the double ring galaxy NGC 7098. It was studied in detail by the ROTASE model in reference [17], however, it is a very important representative galaxy with well-defined double ring pattern, it will be re-described here. This galaxy is classified as (R)SAB(rs)a, and is described on Wikipedia as a smaller inner ring wrapped around the galactic bar and a big well-defined outer ring located outside of the inner ring. This seems to be the most accepted description in the astronomy community. The galactical bar lines up with minor axis of the ring pattern. However, upon further inspection of the image, one can find that the outer ring and the inner ring are connected at the area near the ends of galactic bar marked by C and E in Figure 12e. These connections have very smooth spiral characteristics connecting the inner ring to the outer ring, and is highly symmetric with respect to the galactic center. Buta noticed this interesting phenomenon and marked "The outer ring is complicated by the emergence of spiral structure from its minor axis region, and I believe what we are seeing in this case is an R1R'2 morphology where the R'2 component is not as fully developed as in NGC 1079 and 3081" [26]. The ROTASE model gives a completely different explanation for the formation of this galaxy, where the special connection clearly reveals how the outer rings are developed. The double ring pattern can be well simulated by the ROTASE model shown in 12e with the parameter ϱ following the Gaussian equation:

$$\rho = 0.55 * \exp\left(-0.0001 * (\theta - 360)^2\right) \quad (24)$$

The parameter ϱ equation (24) indicates that the peak emission of the X-matter by the SMBH occurred at 360° of galactic bar rotation time in the past from current. The result from the ROTASE model shows that the double ring pattern is actually made of two identical rings, and each ring is made of a half inner ring and a half of outer ring, each ring crosses other ring twice with arm crossing style very similar to the chain-link two rings, which is clearly illustrated in the reference paper [17], and will not be repeated here to avoid unnecessary overlap of contents. Therefore, this type of the double ring patterns like NGC 7098 can be named as chain-link double ring pattern.

The parameter k in the equation (23) is very important, because it will significantly impact the morphology of the chain-link galaxies. When the parameter k gradually reduces to zero, the chain-link double ring pattern will gradually approach to the single spiral ring pattern and the difference between the major axis and minor axis of the pattern will gradually decrease to zero, so the single spiral ring patterns like CGCG 119-82 and listed in Figure 10 are the special cases of double ring patterns with two identical rings perfectly overlapped together, and as clearly illustrated in reference [17].

Figure 12b is the UGC12646, which is a well-defined double ring galaxy with chain-link arm crossing style, its galactic bar lines up with its minor axis and is another good representative studied by ROTASE model in detail in reference paper [17]. The double ring pattern can be well simulated shown in Figure 12f with the parameter ϱ following the Gaussian equation:

$$\rho = 0.655 * \exp\left(-0.00013 * (\theta - 360)^2\right) \quad (25)$$

The peak emission of the X-matter by the SMBH is also at 360° of bar rotation time in the past from now. This galaxy clearly show that the luminosity and the quality of the spiral arms sequentially decreases along the arm lines from the ends of galactic bar, the ROTASE model offered a clear explanation that such sequential decrease along the arm lines which is due to the gradual decrease of the amount of extra hydrogens converted from the X-matter, the age and the density of stars in the arm areas have little or no effect on the sequential decrease of the luminosity and the arm quality [17]. Other available models cannot clearly explain such sequential decrease. Please refer to the reference paper for the detail analysis by the ROTASE model.

Preprints (www.preprints.org) | NOT PEER-REVIEWED | Posted: 1 September 2021 doi:10.20944/preprints202109.0004.v1

Figure 12c is the original image of galaxy NGC 2665 with double ring pattern with chain-link arm crossing style, its galactic bar lines up with its minor axis. It can be nicely simulated by the ROTASE model shown in Figure 12g with the parameter ϱ following the Gaussian equation:

$$\rho = 0.65 * \exp\left(-0.0001 * (\theta - 360)^2\right) \quad (26)$$

The peak emission of the X-matter by the SMBH is at the 360° of bar rotation time in the past from now. The X-matter emission of NGC 7098, UGC12646 and NGC 2665 seems happened almost at the same time with the same emission behavior.

Figure 12d is the original image of SDSS J015701.50-001644.4 with double ring pattern. The morphology of this galaxy shows the chain-link double ring pattern, but the galactic bar does not line up with the minor axis, nor does it line up with the major axis of the ring pattern as shown in the simulation by the ROTASE model shown in Figure 12h with parameter ϱ following the Gaussian equation:

$$\rho = 0.65 * \exp\left(-0.0001 * (\theta - 410)^2\right) \quad (27)$$

The peak emission of the X-matter by the SMBH is at 410° of galactic bar rotation time in the past from now, which is about 50° rotation time ahead of NGC 7098, UGC 12646and the NGC 2665. The minor axis is about 50° from the galactic bar. The major axis of outer ring is about 40° from the galactic bar. It cannot be classified by Buta's classification as either R1′ subclass (as defined as 180 ° winding relative to the bar axis) or R2′ subclass (as defined as 270° winding relative to the bar axis)[27]. It is instead between R1′ and R2′, but not exactly a mix of the R1′ and R2′ either. It is a very special morphology. The arm crossing points C and E are not located at the Lagrangian points L1 and L2 or other Lagrangian points L4 and L5 in the Manifold model. The dark spaces of this galaxy are not located at the L4 and L5 Lagrangian points which does not match Buta's interpretation [28]. The image of this galaxy shows that the luminosity sequentially decreases along the arm lines with outer rings almost fading away. If the galaxy continues evolving with the same trend, the outer ring will disappear in the future and become a galaxy with its morphology similar to CGCG 119-82 above. The ROTASE model is able to produce a pattern that fully matches the current morphology.

9.3. Galaxy J102942.99-022704.0 with 8-shaped unequal double rings

The original image of the galaxy J102942.99-022704.0 is shown in Figure 13 left, the quality of the image is not high, but it still clearly shows the 8-shaped double ring pattern with unequal double rings, the two rings are very unsymmetrical, the south ring (yellow) is much narrower than the north ring (red),

Figure 13, Galaxy J102942.99-022704.0, left: original image, right: the simulation by ROTASE model, Euler (-47,0,0,)

Preprints (www.preprints.org) | NOT PEER-REVIEWED | Posted: 1 September 2021 doi:10.20944/preprints202109.0004.v1

The unusual pattern can be nicely simulated by the ROTASE model with the following parameter ϱ equations:

$$\rho = 0.6 * \exp\left(-0.0001 * (\theta - 380)^2\right) \quad (28)$$

for the north ring (red), and

$$\rho = 0.6 * \exp\left(-0.00025 * (\theta - 360)^2\right) \quad (29)$$

for the south ring (yellow). Apparently, the X-matter emissions at the two sides of the SMBH are not equal which caused such unequal 8-shaped double ring pattern.

9.4. *Type III: Galaxies with 8-shaped double spiral-ring wrapped with a larger outer ring*

This type of ring patterns is much more complicated than type II galaxies. Figure 14 shows 4 galaxies with such complicated ring patterns. The top row is the galaxy NGC 1079, it was studied by the ROTASE model in previous paper [17], the left is the original image, and the middle is the pattern profile depicted by Buta and the spiral ring pattern is classified as R1R2′ mix pattern by Buta [28]. The right is the simulation by the ROTASE model with the parameter ϱ following the Gaussian equation:

$$\rho = 0.6 * \exp\left(-0.000015 * (\theta - 450)^2\right) \quad (30)$$

Its major axis lines up with the galactic bar and the minor axis is perpendicular to the galactic bar. The peak emission of the X-matter by SMBH is at 450° of galactic bar rotation time in the past from now. The simulation shows that the complicated ring pattern is actually made of two identical rings. For red line arm, it stars at bar end A, extends to B the, to C, then to D, at D it crosses the yellow line arm, then extends to outer ring E, then extends to F, at F it crosses the yellow line again, then extends back to C, crosses itself at C, therefore, each ring is made of a half outer ring and multi section inner rings, each ring crosses other ring twice and cross itself once. Such interesting arm crossing can only be revealed by the ROTASE model at the moment.

The Figure 14 middle is the galaxy 3081, left is the original image, middle is the spiral ring pattern profile depicted by Buta [29] and the right is the simulation of the Disk-subtracted B-band image [30] by ROTASE model with parameter ϱ following the Gaussian equation:

$$\rho = 0.6 * \exp\left(-0.000015 * (\theta - 450)^2\right) \quad (31)$$

The characteristics of the pattern should be the same as the NGC 1079, will not be repeated here.

The Figure 14 bottom are the depicted pattern profiles of ES 509-98 and ESO 507-16 by Buta [26], they all have R1R2′ mixed pattern classified by Buta. The ESO-507-16 has the same pattern as the NGC 3081. But the ESO 509-98 seems having irregular R1R2′ pattern, the profile does not have central symmetry, the major axis does not line up with the galactic bar nor perpendicular to the galactic bar. The arm cross-points do not seem to line up with the major axis nor the minor axis. The ROTASE model would interpret this as the X-matter emissions at two sides of the central SMBH are not equal and the parameter ϱ may not exactly follow the Gaussian equation (23).

Preprints (www.preprints.org) | NOT PEER-REVIEWED | Posted: 1 September 2021 doi:10.20944/preprints202109.0004.v1

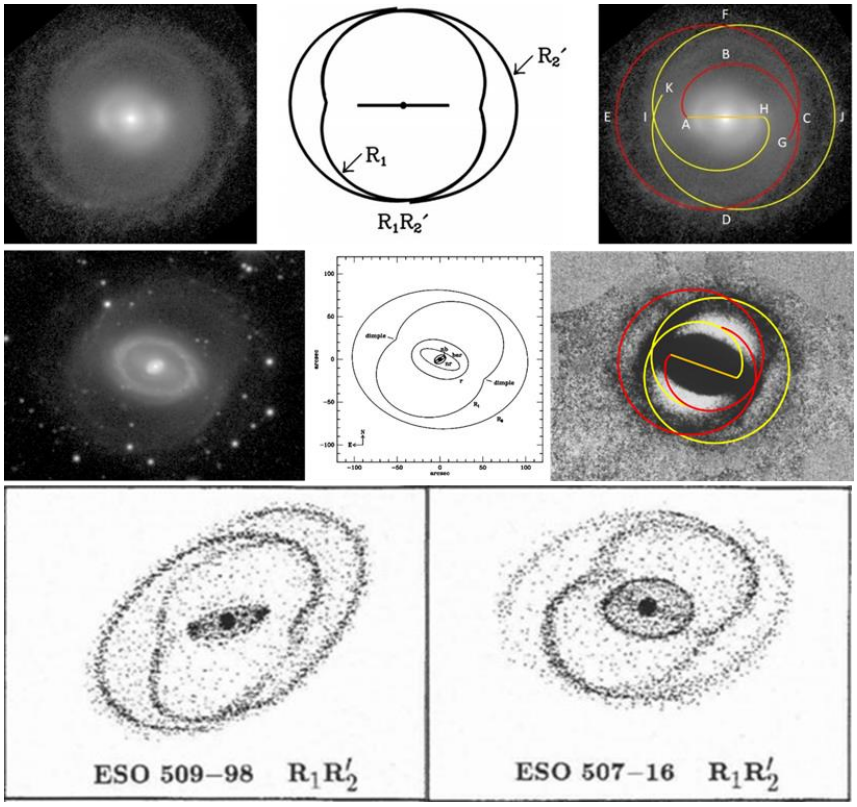

Figure 14, type III ring pattern with 8-shaped inner ring wrapped by a larger outer ring. Top: NGC 1079, left: original image, middle: depicted pattern profile [28], right: simulation. Middle: NGC 3081, left: original image, middle: depicted pattern profile [30], right: simulation, Euler(-20,5,40). Bottom: pattern profiles depicted by Buta [26], left: ESO 509-98, right: ESO 507-16

9.5 *Type IV: Galaxies with pure ring patterns without spirals and galactic bars*

Hoag's object is one of the most fascinating objects in the sky as shown in Figure 15 left. It has an almost perfect ring dominated by bright blue stars, while near the center lies a ball with much redder stars that are likely much older. Between the bugle and the ring is a gap that appears almost completely dark. The Figure 15 right is the galaxy ISI961159, which looks like a twin of Hoag's object. We have to admire the nature's super power to create such beautiful artworks.

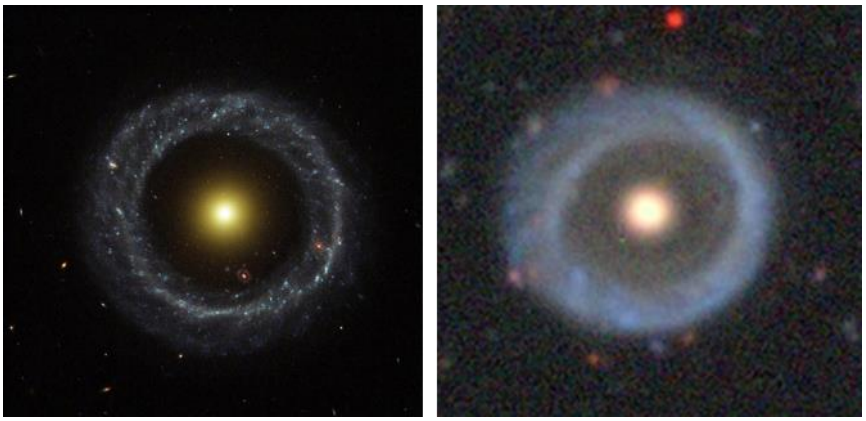

Figure 15. left: Hoag's object; right: ISI961159

The mechanism for the formation of the Hoag's object is still not clear. One theory believes that it is the gravitationally lensed image of a background galaxy[31]; the other

Preprints (www.preprints.org) | NOT PEER-REVIEWED | Posted: 1 September 2021 doi:10.20944/preprints202109.0004.v1

theory proposed that the rotation speed of the galactic bar gradually increases to a certain point that the bar structure is not stable and breaks down to spirally spin-out, the density waves are migrated out into a ring-structure which may be called a resonance ring. Galactic materials will accumulate in the ring area by pressure and gravitational force to promote new star formation, and a spherical bugle is leftover at the center with redder and older stars [32]. The possible collision between galaxies may produce this ring structure also [33, 34]. Schweizer and et. al., studied Hoag's object with photometric and spectroscopic observations, and their findings ruled out the all those three hypotheses. They proposed a new hypothesis of accretion with mass transfer between galaxies, and this accretion event took place at about 2-3 Gys ago [35].

However, the ROTASE model will give a different explanation for the formation of Hoag's object. From the galaxies MCG+00-04-051 and M51 above, we learned that the X-matter emission by the central SMBH can change at any time in any format. For galaxies with a spiral ring pattern like CGCG 119-82, ESO-325-28, and NGC 2273 above, if the X-matter emission is completely terminated by the central SMBH, the X-matter emitted before the termination will continue to spiral outwardly into the ring and the extra hydrogens in the bar will be depleted. The spirals will disappear and the bar will gradually shrink from a bar to a US football-like egg shape. The galactic bar will further shrink and eventually will become a spherical ball bugle at the center with redder and older stars due to depletion of the extra hydrogens; the X-matter in the ring will continue to be converted to hydrogens to refuel the local stars and promote new star formation. Therefore, only the ring and the central bugle will be visible like the current Hoag's object. The explanation by ROTASE model is supported by the morphologies of NGC 1291 and NGC 6028 shown in Figure 16.

Figure 16, Left: NGC 1291; right: NGC 6028

Both NGC 1291 and NGC 6028 are barred galaxies without spiral structures. However, with a rough visual estimate, the length of the bar is about half of diameter of the ring for NGC 1291, and the length of bar is about a quarter of the diameter of the ring for the NGC 6028, as marked by red lines in the images. This indicates that the bar of NGC 1291 is in the early stage of bar shrinking. It has already shrunk to an egg-shaped bar, and the spirals have disappeared. The galactic bar of NGC 6028 is in late stage of shrinking. It will disappear soon and become a true Hoag's object galaxy. Therefore, both galaxies are excellent examples of intermediate galaxies for the transition from spiral ring galaxies to Hoag's objects and solid support for the ROTASE model.

Preprints (www.preprints.org) | NOT PEER-REVIEWED | Posted: 1 September 2021 doi:10.20944/preprints202109.0004.v1

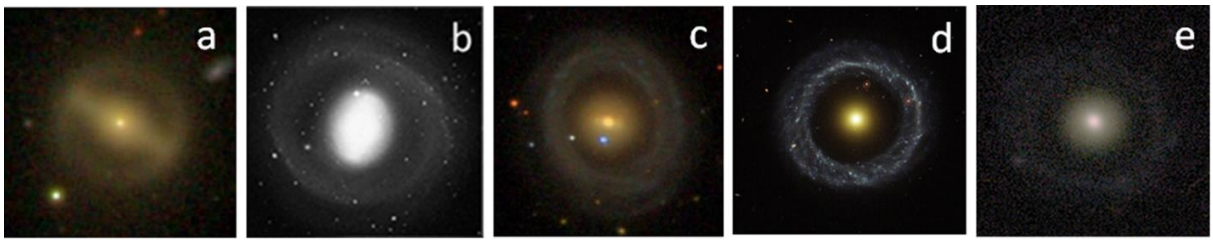

Figure 17, the possible evolution sequence of the Hoag's object from a to e.
a: CGCG 119-82, b: NGC 1291, c: NGC 6028, d: Hoag's object, e: J084119.22+271036.2

If the galaxy evolves with the same trend, i.e., the black hole will not resume the X-matter emission in the near future, the ring and bugle will be dimmer and dimmer like the galaxy J084119.22+271036.2 shown in Figure 17e, in which the outer ring is barely visible. It will be eventually invisible due to complete depletion of the extra hydrogens and temperature decrease of the bugle, but the galaxy still exists like an invisible ghost wandering in the universe. The universe should have a lot of dark/invisible galaxies wandering around which may collide/merge with other galaxies. Figure 17 shows the possible evolution sequence of the Hoag's object from Figure 17a to Figure 17e. The formation of the Hoag's object is just a natural consequence predicted by the ROTASE model when the X-matter emission is terminated for a galaxy with the single spiral-ring pattern.

10. Galaxy 4618 with one spiral arm

The results of the galaxy MCG+00-04-051 and NGC 4548 show that the X-matter emission behavior of the central SMBH can change in any format and at any time. The emissions at the two sides of the SMBH can be also unequal. It will be naturally concluded by ROTASE model that a galaxy may have only one arm if one side has weak or no X-matter emission but other side has strong X-matter emission. The famous NGC 4618 is one of these one-arm galaxies. The luminosity sequentially decreases along the arm line shown in Figure 18 left. Kaczmarek and Wilcots studied in detail about NGC 4618 and ruled out the possible mechanism for the formation of the one-arm galaxy by the gravitational interaction between NGC 4618 and NGC 4625 [36]. Therefore, a one-arm galaxy must be formed by an internal process that is still unclear so far. The one arm spiral pattern of NGC 4618 can be simulated nicely shown in the Figure 18 middle by the following parameter ϱ equation with 505° rotation angle:

$$\rho = 0.65 * \exp\left(-0.000025 * (\theta - 415)^2\right) \quad (32)$$

Figure 18, NGC 4618 with one spiral arm and simulation, Euler(10,0,0)

The parameter ϱ equation (32) matches the general parameter equation (23) for ring galaxies. The one spiral arm is a truncated ring pattern, and the NGC 4618 galaxy would be a perfect 8-shaped chain-link double ring galaxy if it had the other ring as shown in Figure 18 right with yellow dash line. The cross points would be at locations A and B. Due

Preprints (www.preprints.org) | NOT PEER-REVIEWED | Posted: 1 September 2021 doi:10.20944/preprints202109.0004.v1

to the symmetry of A and B with respect to the galactic center, the density and the ages of stars as well as the physical environment in A and B areas should be more or less the same, but the luminosity of area A is much stronger than area B. This stronger luminosity in area A reflects brighter stars and more new star-forming activities, which requires much more hydrogens. Why does area A have much more hydrogens than the area B? The ROTASE model seems the only one to give a logical and natural explanation at the moment. The pattern of the NGC 4618 perfectly matches the ROTASE model and is a good solid support for the model.

11. Possible description of the evolution of the spiral pattern by the ROTASE model

Based on the ROTASE model, the spirals of the galaxies are developed from the inside out in time sequence. This provides a possibility to project the possible spiral pattern evolution of the galaxies as illustrated with the galaxies UGC 6093 and M51.

11.1 *The possible spiral pattern evolution of the galaxy UGC 6093*

The spiral pattern of UGC 6093 can be nicely simulated shown in Figure 19. The image of the galaxy shows clearly three distinguishable development stages by yellow, red and blue lines, respectively. The blue line section is simulated by the following parameter ϱ equation for the galactic bar rotation angle 0° to 270°:

$$\rho = 0.85 * \exp\left(-0.000015 * (\theta - 500)^2\right) \tag{33}$$

The red line section is simulated by the following parameter ϱ equation for the galactic bar rotation angle 271° to 470°:

$$\rho = 0.384 + 0.0012 * (\theta - 270) \tag{34}$$

And the yellow line section is simulated by the following parameter ϱ equation for the galactic bar rotation angle 471° to 575°:

$$\rho = 0.624 * \exp\left(0.002 * (\theta - 470)\right) \tag{35}$$

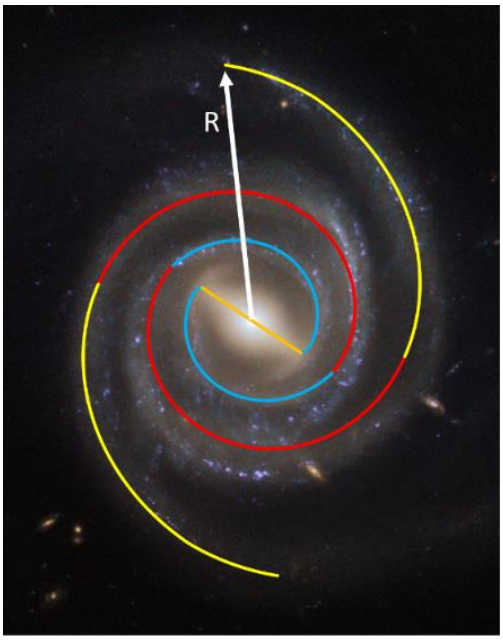

Figure 19. Three section simulations for UGC 6093, Euler (57, 0, 0)

Preprints (www.preprints.org) | NOT PEER-REVIEWED | Posted: 1 September 2021 doi:10.20944/preprints202109.0004.v1

Please remember that the ϱ is the ratio of the X-matter emission velocity out of the confined route over the disc flat rotation velocity. Therefore, a change in ϱ with time means the X-matter emission velocity changes with time. If ϱ increases with backward time, this means that the X-matter emission was larger in the past. Here, the rotation angle θ is equivalent to the evolution time scale. Figure 20 shows the parameter ϱ change with time from past to current time. The ϱ has been continuously decreasing from 575° galactic bar rotation time ago to now. This means that the X-matter emission by the central SMBH has been continuously decreasing during this time period, and the central SMBH may gradually evolve to a new stage.

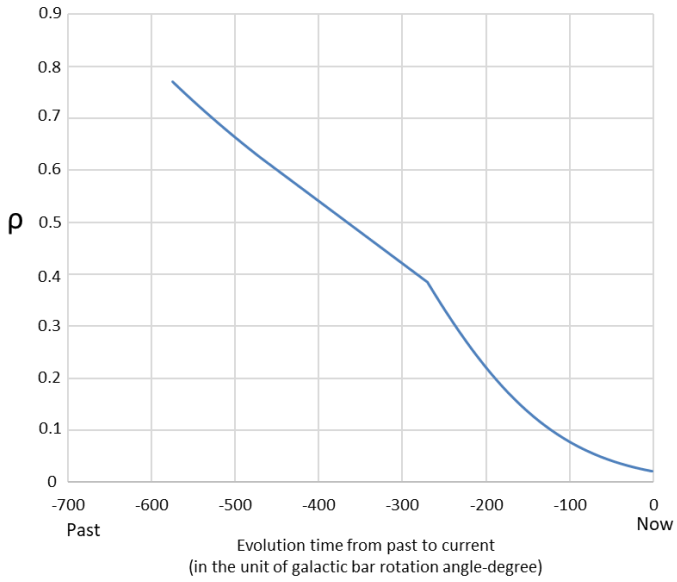

Figure 20. Parameter ϱ change with evolution time of the galaxy UGC 6093

The R in Figure 19 is the radius of the maximum visible spiral arm in this image and will be used as a reference size of the galaxy during the illustration of its spiral pattern evolution. The two opposite entirely visible arms show almost perfect winding symmetry with respect to the galactic center in each different development stage (yellow, red and blue). This continuous change of the morphology with perfect central symmetry must have happened internally, because if such change was caused by external impacts (like other galaxies or objects), then there would have to be two forces that were separate, simultaneous, opposite, and identical in intensity and time. It is likely impossible that such perfectly collaborative impacts would happen simultaneously. According to the Density Wave Theory, the spiral arms are density waves which are initiated by instability [14, 37]. If the instability happened in the non-central locations, could the instability produce such perfectly centrally-symmetric long arms with nice winding in nature? Most likely, the possibility is zero. It is much more reasonable to believe that the arms were produced at the ends of galactic bar and swirled outwardly as in the ROTASE model proposed.

The current spiral pattern of the galaxy UGC 6093 was developed sequentially in time based on the parameter ϱ equations (33), (34) and (35). Therefore, the spiral patterns at different stages of evolution have different morphologies. It is possible to describe the entire evolution of the spiral pattern with the ROTASE model with a certain time range, while there is no such equivalent method from other current available models. The principle behind this model is equivalent to the motion of an object in Newtonian physics: the past and future motion of the object can be calculated based on its current motion by Newton's laws of motion. Figure 21 shows the possible spiral pattern evolution of the UGC 6093 from the near past to the near future calculated by the formulas with assumption that the structure and the rotation of the galaxy is stable during such time period.

Preprints (www.preprints.org) | NOT PEER-REVIEWED | Posted: 1 September 2021 doi:10.20944/preprints202109.0004.v1

Figure 21A is the possible past spiral pattern of UGC 6093 at 470° galactic bar rotation time from current time (roughly about 135 million years ago if using the rotation of the galactic bar of the Milky Way as a reference). At that time in the past, the blue and red line sections had not started yet, and the spiral arms were produced with parameter equation:

$$\rho = 0.624 * exp(0.002 * \theta) \quad (36)$$

The total rotation angle of the galactic bar is 240° with assumption that the maximum radius of the visible spiral arms is the same as the current radius R shown in Figure 19.

Figure 21B is the possible past spiral pattern of UGC 6093 at 270° galactic bar rotation time from current time (roughly about 80 million years ago), at that time in the past, the blue line section had not started yet.

Red section with θ (0° to 200°): $\rho = 0.384 + 0.0012 * \theta$ (37)

Yellow section with θ (201° to 350°): $\rho = 0.624 * \exp(0.002 * (\theta - 200))$ (38)

Figure 21C is the current spiral pattern of the UGC 6093.

Figure 21D is the possible future spiral pattern of UGC 6093 at 150° galactic bar rotation time from current time with 1.5 loop windings (roughly about 45 million years future),

Blue section with θ (0° to 420°): $\rho = 0.85 * \exp(-0.000015 * (\theta - 650)^2)$ (39)

Red section with θ (421° to 620°): $\rho = 0.384 + 0.0012 * (\theta - 420)$ (40)

More or less in 150° of the galactic bar rotation angle time range in the future, only blue and red sections will be visible, the yellow section arms will fade away and disappear due to aging. This projection is based on the fact that current visible spiral galaxies have less than two loop windings, and most long arm galaxies have 1 to 1.5 loop windings. The UGC 6093 will be more tightly wound with smaller visible radius of the spiral arms.

Preprints (www.preprints.org) | NOT PEER-REVIEWED | Posted: 1 September 2021 doi:10.20944/preprints202109.0004.v1

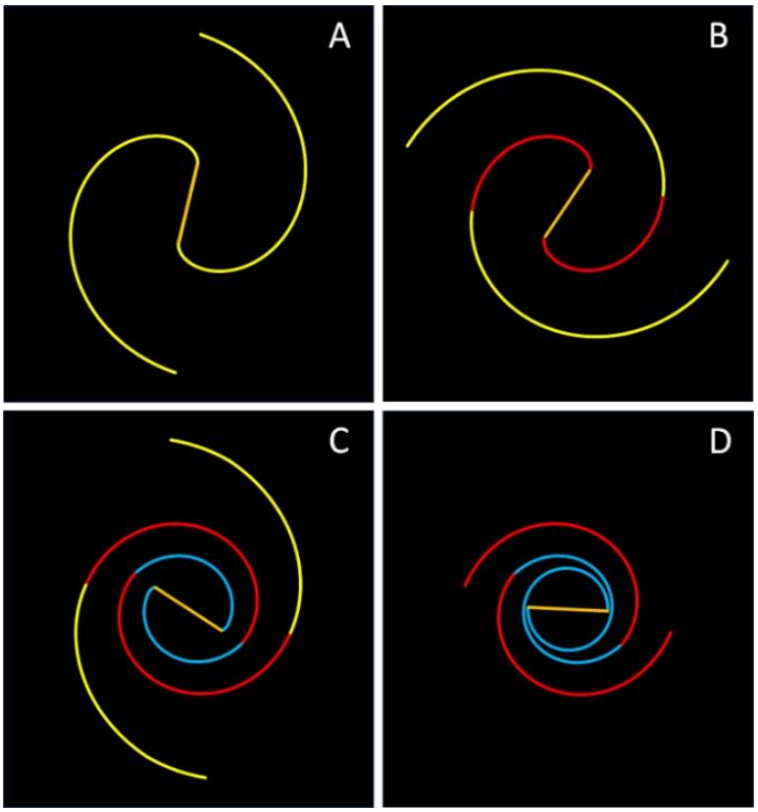

Figure 21. The possible evolution of the spiral arm pattern of UGC 6093. A: 470° of bar rotation angle (time) past; B: 270° of galactic bar rotation angle past; C: Current; D: 150° of galactic bar rotation angle (time) future.

Figure 21 shows that the spiral pattern of the galaxy UGC 6093 may have been changing continuously during the entire history of its evolution. If the length and curvature of the spiral arms change with the evolution of the galaxy, then its pitch angle should follow such a change also. Figure 22 shows the pitch angle change with the evolution calculated from the Figure 21. One can see that its pitch angle decreases significantly along the evolution time line. The average pitch angle of a galaxy also depends on the quality of the image. For example, for NGC 4548 shown in Figure 13, the pitch angles from those two different images will be significantly different. It was clearly demonstrated that the pitch angle of a galaxy heavily depends the length of the spiral arm [18]. The quality of an image heavily depends on how the image is taken such as the wavelength, the photographic exposure time, etc. Such significant dependencies cast a doubt on the possible relationship between the calculated pitch angle of the galaxy and the mass of SMBH and its reliability. The SALWA pitch angle of the one arm galaxy NGC 4618 is 10.62°, does the pitch angle represent the entire galaxy? It is expected that the average pitch angle of galaxies in Hoag's object family (such as the galaxy ISI961159, galaxies in Figure 18) should be zero or almost zero. The galaxy CGCG 119-82 studied in section 8.5.1 above has a very tight ring pattern with a strong galactic bar, and the average pitch angle of this type of galaxy with the tight ring pattern is expected to be almost zero. There is no justification to claim that zero pitch angle correlates to the mass of a "super-super" massive black hole in the galactic center.

Preprints (www.preprints.org) | NOT PEER-REVIEWED | Posted: 1 September 2021 doi:10.20944/preprints202109.0004.v1

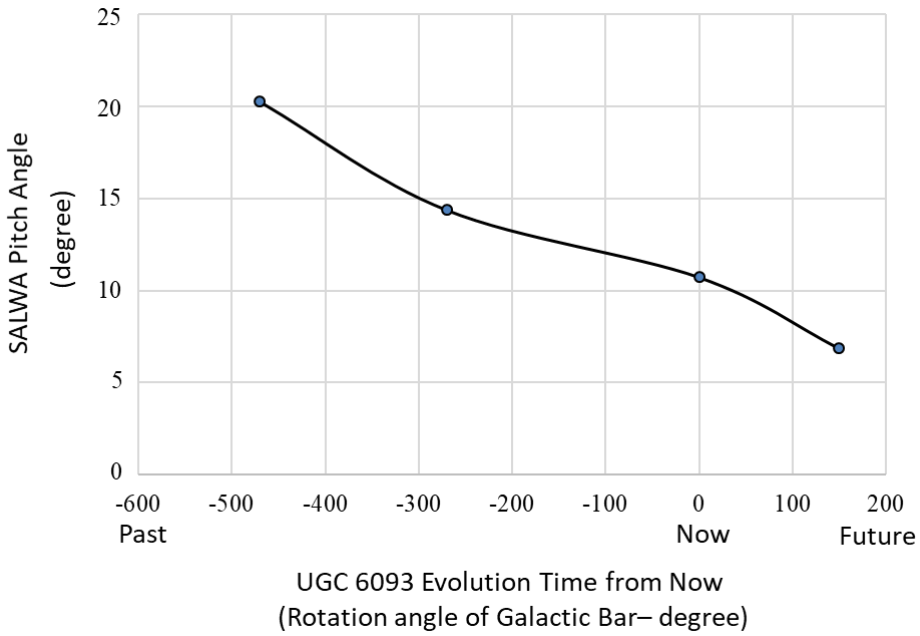

Figure 22. The pitch angle changes with evolution time of UGC 6093

Readers may think that the description of the possible evolution of the UGC 6093 in Figure 21 just parameterizes the spiral curve, splits the curve into different sections and treats each section separately. However, this is a misunderstanding because the mathematical parameterization of a curve and the simulation of the curve by a physical model have fundamental difference although the two methods use the same mathematical procedure. Theoretically and realistically speaking, one can fit any spiral curve with multi-section method by different mathematical equations without a physical model, but such parametrization is just pure mathematics and does not have any physical meaning. When developing parameterized equations from a physical model, all the parameters and variables in the equations have their unique physical meanings and will describe the characteristics of the curve for why and how. For example, the trajectory of a bullet shot from a gun can be easily fit by many mathematical equations with multiple sections, but such fitting is just a pure mathematics and has no any physical meaning. Only the fitting (or parametrization) by the Newton's law of motion has real physical meaning such as the speed, direction, gravity, wind speed, air friction, distance, etc.

As an illustration, the new spiral formulas derived from this ROTASE model can be used to simulate the spiral patterns of Earth natural spiral objects as shown in Figure 23.

Preprints (www.preprints.org) | NOT PEER-REVIEWED | Posted: 1 September 2021 doi:10.20944/preprints202109.0004.v1

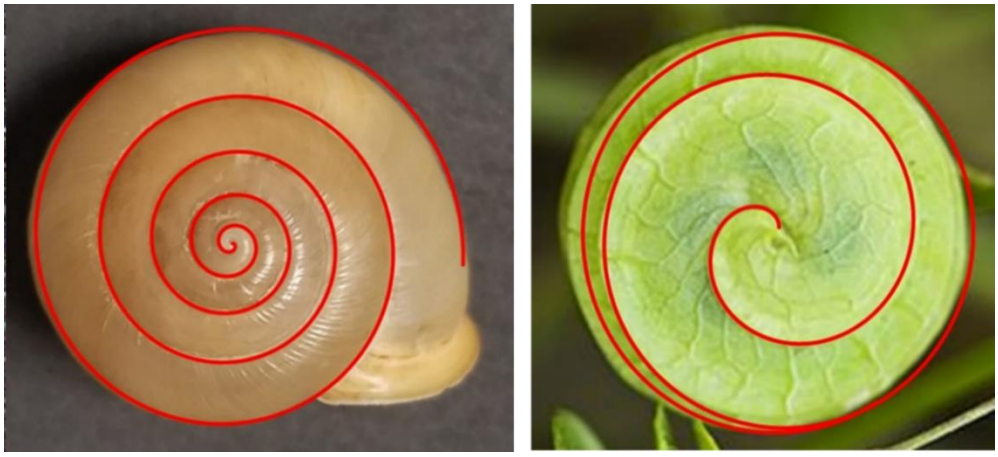

Figure 23, Simulation of spirals of land snail shell (left) and the Medicago Orbicularis seed pod (right) by ROTASE model.

The spiral pattern of the land snail shell can be nicely simulated with the following parameter equation:

$$\rho = 2 * (1 + 0.0011 * \theta) \tag{41}$$

And the spiral pattern of the Medicago Orbicularis seed pod can be nicely simulated with the following parameter equation:

$$\rho = 4 * \exp(-0.001 * \theta) \tag{42}$$

However, the simulation in Figure 23 is just pure mathematics without any physical meanings.

The 3-section simulation of the UGC 6093 in Figure 19 clearly indicates the time sequence that the yellow section was developed first, then, the red section, and the blue section is last (current). The time sequence is the evolution sequence, so we can roughly know what the spiral pattern looks like when only the yellow section was developed, what the spiral pattern looks like after the red section and yellow section were developed and so on. However, this type of description of the possible evolution of the spiral pattern is limited to the available time sequence associated to each section for any galaxies. We cannot deduce the possible spiral pattern in the past before the yellow section and future pattern too far from the current pattern.

11.2 *The possible spiral pattern evolution of the Galaxy M51*

As shown by the original image of M51 and the simulation in section 8.2, the M51 has two very distinguishable spiral development periods by the yellow and red spiral lines. In time sequence, the yellow spiral lines were developed first, the red spiral lines were developed later. The past spiral pattern of M51 at 485° of galactic bar rotation time in the past is shown in Figure 24 in which only the yellow arms were developed and the red spiral arms had not started yet. The parameter ϱ equation for this period of time is:

$$\rho = 0.00088 * (\theta - 50)^2 + 11.704 \tag{43}$$

Preprints (www.preprints.org) | NOT PEER-REVIEWED | Posted: 1 September 2021 doi:10.20944/preprints202109.0004.v1

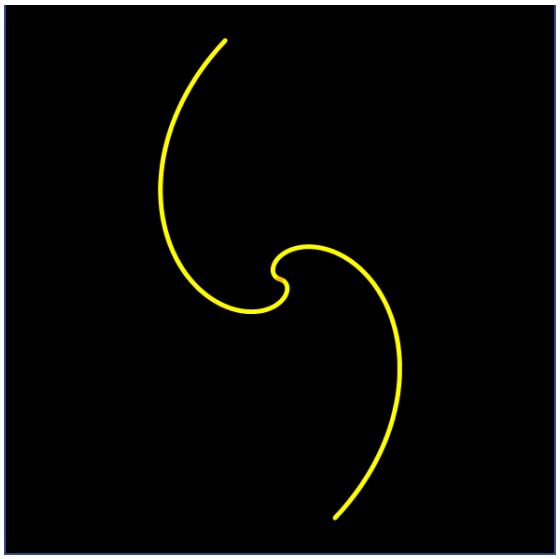

Figure 24, the possible spiral pattern of the M51 at 485° of galactic bar rotation time in the past from now.

We cannot project the spiral pattern of M51 before the yellow line without some reliable clues (or references). Furthermore, if the M51 and its companion galaxy NGC5195 continue to move closer in the future, then, it will be expected that the yellow line spiral arm will gradually fate away due to aging, but the central symmetry of M51 will be further damaged by the increase of highly unsymmetrical gravitational interaction between the two galaxies.

12. Milky Way

The Milky Way is the galaxy in which we reside. There is no way we can get a real image of the whole Milky Way, and the most recent available image is an artist's illustration as shown in Figure 25. The illustration is based on clues from many observations and comparison of such observations with other galaxies. Whether the real morphology of the Milky Way matches the illustration is a question. Based on the illustration, the Milky Way is a barred spiral galaxy with two major leading spiral arms and two minor branches. The two major spiral arms can be nicely simulated shown in Figure 25 by the ROTASE model with the following parameter equation:

$$\rho = 0.18 * (1 + 0.0085 * \theta) \tag{44}$$

The SALWA pitch angle of the Milky Way is about 12.33°. However, the reliability of this value will depend on the reliability of the artist's depiction of the Milky Way. This pitch angle is about half of the value obtained by Levine et. al. [38], but agrees very well with most of data listed in Vallée's paper [39]. If the illustration roughly reflects the main characteristics of the true Milky Way, then, the parameter ϱ equation (44) indicates that the X-matter emission in the Milky Way is relatively weak and steadily decreases. The spiral arms will be more tightly wound in the future if the current trend continues, such information can only be revealed by the ROTASE model at the moment. While this may indicate that the visible spiral arm size of Milky Way disc could be smaller in the near future, but this does not mean that the real disc size will be smaller.

Preprints (www.preprints.org) | NOT PEER-REVIEWED | Posted: 1 September 2021 doi:10.20944/preprints202109.0004.v1

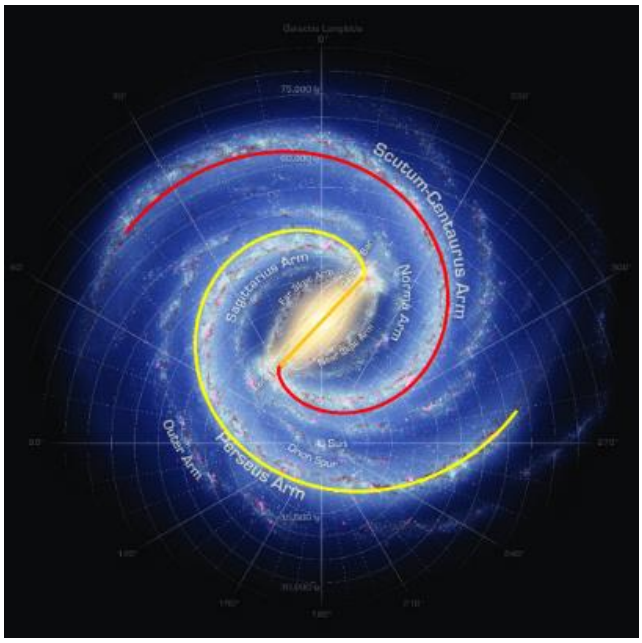

Figure 25, Milky Way and simulation by the ROTASE model, Euler (43, 0,0). $\rho = 0.18*(1+0.0085*\theta)$

13. Comparison with other spiral equations

The Archimedean spiral, hyperbolic spiral, Logarithmic spiral and Ringermacher-Mead spiral are commonly used to fit spiral patterns of galaxies [40-44]. The Archimedean spiral produces spirals with equal space between the spiral windings; the hyperbolic spiral has very flat/straight line when the rotation angle is small, the curvature of the spiral gradually increases with the increase of the rotation angle; the logarithmic and Ringermacher-Mead spirals have similar characteristics which produce nice spirals when the rotation angle is small, and the spirals will gradually become flat and approach an asymptotic straight line when the rotation angle increases. The Archimedean, hyperbolic and the logarithmic spirals are limited to a very small portion of spiral galaxies; the Ringermacher-Mead spiral has much broader application with two adjustable parameters. However, all these spiral formulas cannot produce the ring patterns like Figure 1a, Figure 1b, Figure 1f and Figure 1g, and cannot quantify the radius of the ring equivalent to equation (8). In addition, fitting spiral pattern with all those formulas is just pure mathematics without any physical meaning.

14. Discussion

The ROTASE model successfully describes the spiral galaxies in many aspects as demonstrated above, and the accurate simulation of the ring patterns is really a miracle. It assumes that the mysterious unknown X-matter is emitted by the SMBH, and this assumption is a conjecture based on many characteristics of the spiral galaxies. The hypothesis proposed that this X-matter cycles in the universe. In this cycle, the gravitational matter accumulates in the SMBH and is converted to the X-matter with non-gravitational or anti-gravitational property inside of the SMBH with an extremely unimaginable physical environment. Then the X-matter is converted to gravitational hydrogens and possible other matters after emission by the SMBH, and these hydrogens will be converted to other matter by fusion. Some or all of this matter may fall back into the SMBH later. The conversion process of X-matter to hydrogens could be "similar" to the matter conversion process in the Big Bang theory, where the primordial matter released during the Big Bang was converted to the hydrogens. The "similar" here does not means in any aspect that the conversion of the X-matter into hydrogens is the smaller scale of the matter conversion in the Big Bang. The physical conditions (such as pressure, temperature, density, etc..) in the

 doi:10.20944/preprints202109.0004.v1

two conversion processes are completely incompatible. This model is in a primary stage and may have many defects and is far from completed. Many new questions may arise. At current stage of physical theories, the black hole has only three externally observable classical parameters (no-hair theorem): mass, electric charge, and angular momentum. Nothing within its horizon can escape from the black hole. The assumption of the X-matter emission by the SMBH directly conflicts with these black hole theories. Critical questions will naturally arise as to how the matter conversion happens inside of the SMBH, and how the X-matter is emitted by the SMBH and later converted to the hydrogens after the emission. There are no answers to those questions currently. Future research by astronomers, cosmologists, high energy physicists and particle physicists may provide answers or never have answers.

The Big Bang theory was proposed 100 years ago. It was highly speculative at that time without explanation for why and how it happened: if the primordial matter released from the Big Bang in the very beginning had mass or was massless; if that matter was gravitational, non-gravitational, or antigravitational; and how the primordial matter was converted to hydrogens and other matters which are the building materials for our universe today. However, after several decades of debate and research with dramatic advancement in high energy physics and particle physics, it has become the leading hypothesis for the universe. Scientists came up with hypotheses to figure out the possible mechanisms for how the initial primordial matter released from the Big Bang was converted to leptons and quarks, and further converted to atoms and started the formation and evolution of stars and galaxies, etc. Understanding the conversion mechanism of X-matter to hydrogens may be more difficult and take more time. Hajdukovic proposed a very interesting hypothesis in which the extremely strong gravitational field deep inside the horizon of the SMBH can create particle-antiparticle pairs from a physical vacuum. The matter and antimatter are repulsive deep inside of the SMBH, and the SMBH violently repels the antiparticles with antigravity force. The universe is in cycling alternatively by matter and antimatter [45]. The matter cycling by the ROTASE model and the hypothesis by Hajdukovic share the same philosophy in different aspects.

The ROTASE model seems consistent with Stephen Hawking's definition. The success of the nice simulation and explanation of various spiral patterns by ROTASE model indicates that everything happens with reasons in the universe; the universe is operated by laws and the mathematics is the execution tool of the laws; the author believes that the spiral patterns of galaxies should be developed by one mechanism not by many mechanisms for the objects with such cosmological scale. This is philosophically consistent Einstein's principle of simplicity.

It is no doubt that the successful description of most (if not all) spiral galaxies by the new set of spiral equations is achieved not by a luck, rather by a mysterious connection between the new set of spiral equations and the real mechanism even if the conjecture of X-matter emission by the SMBH is not compatible with current physics at the moment. We feel the sweet smell in the dark, and we need to find out where and what it is. The ROTASE model is based on the conjecture that the unknown matter is emitted by the SMBH located at the galactic center, however, the proposed and popularly accepted SMBH located at the galactic center has been challenged recently by the new study about the geodesic motion of S2 and G2 around the Milky Way galactic center [46], in this interesting study, Becerra-Vergara et. al., proposed that a quantum core of the fermionic dark matter could be located at the galactic center as alternative to the SMBH. Any new findings are good news to make us better understanding the mysterious heart of the galaxy. The X-matter emission is not necessary from the SMBH, it is just emitted by a mysterious special object at the center of the galaxy, such special object can be called as "black hole" or other names in the future. Extraordinary ideas need extraordinary approaches. Science is the exploration of educated conjectures.

 doi:10.20944/preprints202109.0004.v1

15. Summary

The proposed ROTASE model has made the following achievements so far:

1. New spiral formulas have been derived which can simulate (or fit) most (if not all) of spiral patterns of disc galaxies. The spiral formulas have one parameter and one variable. They should be the simplest formulas to describe the spiral arm patterns of disc galaxies for now and for the future.
2. It explained the observation that star formation happens simultaneously in the entire spiral arm, and new stars in those areas have a narrow range of the ages.
3. It explained the sharp front edge and rear trail blurry pattern of the spiral arms.
4. It explained the special pattern with the broken connection of the spiral arms from the ends of the galactic bar, which is due to the termination of X-mater emission.
5. It predicts that the spiral pattern of the galaxy MCG+00-04-051 in the near future will morphologically look as a "normal" spiral galaxy in which the inner ends of spiral arms will "connect" to the ends of galactic bar instead of being further separated, and the galactic bar will overpass the ends of spiral arms which will make the galactic bar look ahead of the spiral arms.
6. It explained the sequential decrease of the luminosity of the spiral arms along the spiral arm lines from the ends of galactic bars to the ends of visible arms. This is due to the gradual decrease of the amount of the X-matter along the spiral arm line. The distance of the arms to the galactic center, the density and the age of stars are not the main factors for such sequential decrease.
7. It explained the observation of multiple arm crossings of ring galaxies, and demonstrated that most (if not all) rings patterns (single ring and double ring) can be described with the universal Gaussian parameter equation. The single spiral-ring pattern is a special case of the double ring pattern in which the two rings are perfectly merged (overlapped) together.
8. An equation was derived from the model to calculate the radius of the rings for the galaxies with single spiral ring patterns.
9. A formula to calculate the pitch angle of spiral arm is derived from this model. The spiral arm length weighed average pitch angle of the galaxy is proposed for more fairly calculating the average pitch angle for the entire galaxy.
10. It is the first to explain that the double ring patterns like NGC 7098 are actually made of two identical rings and each ring is made of a half inner ring and a half outer ring, the two identical rings are linked with chain-link style arm crossing. This chain-link style arm crossing is caused by the significant difference between the amounts of two X-matter bands which are emitted at significantly different times.
11. It explained the galaxy J102942.99-022704.0 with unequal 8-shaled double rings due to the unequal X-matter emissions at two sides of the SMBH.
12. It is the first to explain that the double ring patterns with 8-shaped inner rings wrapped by larger outer rings like NGC 1079 are actually made of two identical rings, each ring is made of a half large router ring and multi-section inner rings.
13. It explained that the formation of the Hoag's object is due to the termination of the X-matter emission of single spiral-ring galaxies, and its possible pattern evolution sequence is illustrated.
14. It explained the formation of one-arm galaxies in which one side of the SMBH has weak or no X-matter emission, but other side has strong X-matter emission.
15. It provides a method to deduce the possible evolution of the spiral patterns of galaxies where spiral arms have distinguishable sections associated with different time periods.
16. The results from the ROTASE model indicate that the average pitch angle of the spiral galaxies heavily depends on the length of the spiral arms and the quality of the images of galaxies. The average pitch angle also changes with the evolution of the galaxies; such dependence will make the attempt to correlate the average pitch angle with the mass of the central SMBH more difficult and unreliable.
17. It indicates that the matter in the universe may be recyclable in some extent.

18. The results from the ROTASE model indicate that the winding of the spiral arms of the Milky Way may become tighter in the future if the current artist's illustration is reliable.

References

1. Conselice C.; Wilkinson A.; Duncan K..; Mortlock, A. The evolution of galaxy number density at z < 8 and its implications, ApJ, **2016**, **830**, 83-99.
2. Hubble, E. The Classification of Spiral Nebulae, The Observatory, **1927**, 50, 276-281.
3. Elmegreen, D.; & Elmegreen, B. Flocculent and grand design spiral structure in field, binary and group galaxies, MNRAS, **1982**, 201,1021-1034.
4. Elmegreen, D.; Elmegreen, B. Arm Classifications for spiral galaxies. ApJ, **1987**, 314, 3-9.
5. McVitte, G.; Payne-Gaoschkin, C. A model of A spiral galaxy, MNRAS, **1951**, 111 (5), 506-522.
6. Lin, C.; Shu F. On the spiral structure of disk galaxies. ApJ. **1964**, 140, 646-655
7. Shu, F. Six Decades of Spiral Density Wave Theory, Annu. Rev. Astron. Astrophys. **2016**, 54, 667-724.
8. Julian, W.; Toomre, A. Non-axisymmetric responses of differentially rotating disks of stars, ApJ. **1966**, 146, 810-830.
9. Romero-Gómez, M.; Masdemont, J.; Athanassoula, E.; García-Gómez, C. The origin of rR1 ring structures in barred galaxies, A&A **2006**, 453, 39–45.
10. Romero-Gómez, M.; Athanassoula, E.; Masdemont, J.; García-Gómez, C. The formation of spiral arms and rings in barred galaxies, A&A, **2007**, 472, 63–75.
11. Athanassoula, E.; Romero-Gómez, M.; Masdemont, J.; Rings and spirals in barred galaxies – I. Building blocks, MNRAS, **2009**, 394(1), 67–81.
12. Athanassoula, M.; Romero-Gómez, M.; Bosma, A.; Masdemont, J. Rings and spirals in barred galaxies – II. Ring and spiral morphology, MNRAS, **2009**, 400(4), 1706–1720.
13. Athanassoula, E.; Romero-Gómez, M.; Bosma, A.; Masdemont, J. Rings and spirals in barred galaxies – III. Further comparisons and links to observations, MNRAS, **2010**, 407(3), 1433–1448.
14. Dobbs, C.; Theis, C.; Pringle, J.; Bate, M. Simulations of the grand design galaxy M51: a case study for analysing tidally induced spiral structure Mon. Not. R. Astron. Soc. **2010**, 403, 625–645.
15. Dobbs, C,; Baba, J. Dawes Review 4: Spiral Structures in Disc Galaxies, PASA, **2014**, Vol. 31, e035.
16. Pan, H. New formulas and mechanism for the spiral arm formation of Galaxies. IJP., **2019**. 7, 73-85.
17. Pan, H. Application of new formulas for the spiral arm formation to selected galaxies with special patterns. A JAA. **2020,** 8, 45-66.
18. Pan, H. Pitch angle calculation of spiral galaxies based on the ROTASE model. IPJ. **2021**, 9, 71-82.
19. Hawking, S. A brief history of time, (Bantam Books, NY, NY), **1998**, pp 10. ISBN 0-553-10953-7.
20. Grand, R. J. J., Kawata D., Cropper M., Spiral arm pitch angle and galactic shear rate in N-body simulations of disc galaxies, A&A, **2013**, 553, A77.
21. Berrier, J. C., Davis B. L., Kennefick D. et al., Further Evidence for a Supermassive Black Hole Mass-Pitch Angle Relation, ApJ, **2013**, 769, 132.
22. Harry I. Ringermacher and Lawrence R. Mead, Simple fit of data relating supermassive black hole mass to galaxy pitch angle, AJ, **2009**, 137, 4716–4717.
23. Seigar, M.; James, P. The structure of spiral galaxies—II. Near-infrared properties of spiral arms", MNRAS. **1998**, 299, 685-698.
24. Walmsley, M. et al.; Galaxy Zoo DECaLS: Detailed Visual Morphology Measurements from Volunteers and Deep Learning for 314,000 Galaxies, **2021**, https://arxiv.org/abs/2102.08414v1
25. Contopoulos, G.; Grosbol, P. Stellar dynamics of spiral galaxies: nonlinear effects at the ¼ resonance, Astron. Astrophys. **1986**, 155, 11-23.
26. Buta, R. Resonance Rings and Galaxy morphology, Astrophys. Space Sci. **1999**, 269–270: 79–99.
27. Buta, R., The catalog of southern ringed galaxies, ApJS. **1995**, 96, 39-116.
28. Buta, R., Galactic rings revisited. II. Dark gaps and the locations of resonances in early-to-intermediate-type disc galaxies, MNRAS. **2017**, 470, 3819–3849.
29. Buta, R.; Byrd, G. A Hubble space telescope study of star formation in the inner resonance ring of NGC 3081. AJ. **2004**, 127, 1982-2001.
30. Buta, R.; Burcell, G. NGC 3081: Surface photometry and kinematics of a classic resonance ring barred galaxy. AJ, **1998**, 115, 484-501.
31. Hoag, A. A., A peculiar object in Serpens, Astron. J., **1950**, 55, 170.
32. Brosch, N., The nature of Hoag's object: the perfect ringed galaxy, Astron. Astrophys. **1985**, 153, 199-206.
33. Toomre, A., in Evolution of galaxies and stellar populations, ed. R. B. Larson and B. M. Tinsley (New Havenn: Yale University Observatory), p 401.
34. Theys, J.C., and Spiegel, E. A., Ring Galaxies II. ApJ., **1977,** 212, 616-633.
35. Schweizer, et. al., The structure and evolution of Hoag's object, AJ., **1987**, 320 454-463.
36. Kaczmarek, J. and Eric M. Wilcots, E., High-resolution H i distributions and multi-wavelength analysis of magellanic spi-rals NGC 4618 AND NGC 4625, The Astronomical Journal, 2012, 144:67 (13pp).
37. Sellwood J.; Carlberg R. Spiral instabilities: mechanism for recurrence, MNRAS. **2019**, 489, 116-131.

38. E. S. Levine,* Leo Blitz, Carl Heiles, The Spiral Structure of the outer Milky Way in Hydrogen, Science, **2006**, 312,1773-1777.
39. Jacques P. Vallée, The Spiral Arms and Interarm Separation of the Milky Way: An Updated Statistical Study, AJ. **2005**, 130, 569-575.
40. Ma J., A Method of Obtaining the Pitch Angle of Spiral Arms and the Inclination of Galactic Discs, Chin. J. Astron. Astrophys., **2001,** 1, 395.
41. Seigar M. S., Kennefick D., Kennefick J., Lacy C. H. S., Discovery of a relationship between spiral arm morphology and supermassive black hole in disk galaxies, ApJ, **2008,** 678, L93.
42. Karachentsev I. D., Karachentseva V. E., Commun. Byurak. Obs., **1967**, 38, 47.
43. Kennicutt, R. C., Jr. The shapes of spiral arms along the Hubble sequence, AJ. **1981**, 86, 1847-1858.
44. Ringermacher H. I., Mead L. R., 2009, A new formula describing the scaffold structure of spiral galaxies, MNRAS, **2009**, 397, 164-171.
45. Hajdukovic, D.S. Do we live in the universe successively dominated by matter and antimatter? Astrophys Space Sci. **2011**, 334, 219–223.
46. Becerra-Vergara, E., Argüelles, C., Krut1, A., Rueda, J., and Ruffini, R. Geodesic motion of S2 and G2 as a test of the fermionic dark matter nature of our Galactic core, A&A **2020**, 641, A34.